Copy 5
RM E51J04

NACA RM E51J04

NACA

RESEARCH MEMORANDUM

FULL-SCALE INVESTIGATION OF COOLING SHROUD AND EJECTOR NOZZLE FOR A TURBOJET ENGINE - AFTERBURNER INSTALLATION

By Lewis E. Wallner and Emmert T. Jansen

Lewis Flight Propulsion Laboratory
Cleveland, Ohio

NATIONAL ADVISORY COMMITTEE
FOR AERONAUTICS
WASHINGTON
December 17, 1951

NATIONAL ADVISORY COMMITTEE FOR AERONAUTICS

RESEARCH MEMORANDUM

2399

FULL-SCALE INVESTIGATION OF COOLING SHROUD AND EJECTOR NOZZLE FOR A TURBOJET ENGINE - AFTERBURNER INSTALLATION

By Lewis E. Wallner and Emmert T. Jansen

SUMMARY

A full-scale ejector cooling investigation was made on a turbojet engine - afterburner installation in the NACA Lewis altitude wind tunnel. Ejector performance was studied at primary exhaust-gas temperatures from 2700° to 3400° R (corresponding to ejector temperature ratios from 2.0 to 5.0), primary pressure ratios from 1.79 to 3.4, secondary air flows up to 29 percent of the primary gas flow, and for diameter ratios from 1.08 to 1.42 and spacing ratios from 0.04 to 1.16. In addition, variations were made in the primary exhaust-nozzle area.

Ejectors with large diameter ratios permit the attainment of high gas-flow ratios, but the jet-thrust losses become prohibitive as the spacing ratio is increased from 0 to 1.16. As the ejector diameter is reduced, the obtainable gas-flow ratio and the thrust loss are reduced. Previous results showing that data obtained at a temperature ratio of 1.0 could not be extrapolated to determine ejector performance at high temperature ratios by the application of the temperature ratio factor to the gas-flow ratios are substantiated by the present investigation.

INTRODUCTION

With the advent of turbojet afterburning, cooling of the afterburner shell became one of the most important operating problems. Cooling is important not only for structural considerations of the afterburner, but also for protection of the airplane frame from the radiant heat of the afterburner shell. One solution to the cooling problem is the use of a cooling-shroud passage with an ejector nozzle through which cooling air is pumped. Some of the important variables which have not been adequately investigated for the design of a full-scale afterburner - ejector installation are: the thrust characteristics with the ejector, the pressures required to pump air through the shroud, the air flows required to cool the shell, and the effects of changes in flight speed.

At present there is a multitude of small-scale ejector data (obtained in tests with cold air) available in the literature (see references 1

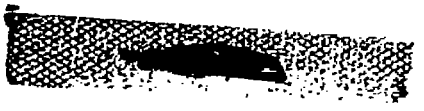

to 3); however, considerable doubt remains as to the applicability of the reference data to actual full-scale designs. The small-scale work of reference 4, for example, indicates a first-order deviation between the corrected data obtained with and without a temperature difference between the primary and secondary jets. As for the effect of ejectors on the jet thrust of a nozzle, the work most commonly referred to is reference 5, which is not applicable to a turbojet afterburning installation.

A full-scale ejector cooling investigation was made on a turbojet engine - afterburner installation in the NACA Lewis altitude wind tunnel. The cooling ejector characteristics were studied at primary exhaust-gas temperatures from 2700° to 3400° R, primary pressure ratios from 1.79 to 3.4, secondary air flows up to 29 percent of the primary gas flow, and for diameter ratios from 1.08 to 1.42 and spacing ratios from 0.04 to 1.16. In addition, variations were made in the area of the primary exhaust nozzle.

The results of the full-scale ejector cooling work done in the altitude wind tunnel at temperature ratios from 2.0 to 5.0 are compared with the relevant small-scale data available in the literature.

APPARATUS

Engine. - The turbojet engine used in this investigation (fig. 1) had a static sea-level thrust rating of slightly over 3000 pounds at a turbine-outlet temperature of about 1200° F. At rated sea-level conditions the air flow is approximately 60 pounds per second.

Afterburner. - The standard tail-pipe of the engine was replaced by an afterburner assembly 80 inches in length (fig. 1), which included a variable-area exhaust nozzle (fig. 2). Details of the afterburner and cooling shroud assembly are shown in figure 3. The afterburner assembly included an annular 2-ring V-type flame holder and an internal cooling liner, which extended from the flame holder to approximately the nozzle outlet, and had a combustion-chamber diameter of 25 inches. In addition, the afterburner was equipped with an external cooling shroud, which consisted of an annular inlet plenum chamber, a cooling-shroud passage 1/2 inch in height (for most of the length) and $48\frac{3}{4}$ inches in length, and a series of ejector nozzles (figs. 3 and 4). At the outlet of the cooling-shroud passage a support ring for the variable-area exhaust nozzle was mounted on the cooling-shroud shell and extended about 40 percent of the distance across the secondary air passage.

[redacted]

Six ejector nozzles (fig. 4), which could be attached to the shroud outlet flange, had the following ejector dimensions:

Ejector configuration	Diameter ratio, D_s/D_p	Spacing ratio, S/D_p
A	1.42	0.04
B	1.42	.79
C	1.42	1.16
D	1.08	.79
E	1.08	1.16
F	1.08	.79

Configuration F differed from configuration D by the addition of a short straight mixing length (see fig. 4).

Installation and instrumentation. - The engine and afterburner assembly were mounted on a wing section which spanned the 20-foot-diameter test section of the altitude wind tunnel (fig. 1). Dry refrigerated air was supplied from the tunnel make-up air system through a duct to the engine inlet. The inlet air duct was connected to the engine by means of a frictionless slip joint which permitted installation drag and thrust to be measured by the tunnel balance scales. Ambient sea-level air was supplied to the cooling-shroud plenum chamber through a duct equipped with a valve used to throttle the air to the desired shroud inlet pressure.

Instrumentation for the engine and afterburner was installed at the stations indicated on figure 3. The locations of the pressure tubes and thermocouples at each of the instrumented stations are shown by the sketches in figure 5.

PROCEDURE

The engine was operated at rated speed and limiting turbine-outlet temperature throughout the investigation. For each ejector-nozzle configuration, the turbine-outlet temperature was maintained constant by varying the afterburner fuel flow to compensate for any change in effective primary exhaust-nozzle area resulting from any effect of the ejector on the primary system. The primary pressure ratio was varied from 1.79 to 3.40. At each primary pressure ratio the cooling-shroud inlet pressure ratio was varied between 0.85 and 2.0, with the limit of the shroud-inlet pressure-ratio range being dependent on the ejector geometry and primary pressure ratio. The data were obtained at a pressure altitude of 30,000 feet with the primary variable-area exhaust nozzle in the full-open position, except for a brief investigation to determine the effect of primary nozzle-area changes on ejector performance.

RESULTS AND DISCUSSION

Basic Ejector Performance Data

Secondary pressure ratio, gas-flow ratio, and jet-thrust ratio are plotted as functions of cooling-shroud inlet pressure ratio (hereafter designated cooling-shroud pressure ratio) at constant values of primary pressure ratio in figures 6 to 11. (See fig. 3 for station locations. The symbols and the parameters are defined in the appendix.)

General ejector performance trends. - For a given primary pressure ratio, increasing the cooling-shroud pressure ratio raised the secondary pressure ratio for all configurations investigated (see figs. 6(a) to 11(a)). The difference between the cooling-shroud and secondary pressure ratios represents the friction pressure loss in the annular cooling-shroud passage surrounding the afterburner shell.

Increasing the cooling-shroud pressure ratio at a given primary pressure ratio also raised the gas-flow ratio, which is the ratio of secondary to primary gas flow (see figs. 6(b) to 11(b)). For the range covered in this investigation, increasing the pressure ratio across the primary nozzle lowered the gas-flow ratio because (1) higher primary gas flows occurred; and (2) expansion of the primary gas flow reduced the effective area of the secondary passage and thus reduced the secondary air flow. The primary gas flow increased from 19 to 35 pounds per second as the primary pressure ratio was increased from 1.79 to 3.40, which was the range covered in this investigation.

The jet-thrust ratio is defined as the ratio of jet thrust of the complete configuration including the ejector to the jet thrust of the primary system alone. For a given primary pressure ratio, increasing the shroud-inlet pressure ratio raised the jet-thrust ratio for all configurations investigated except configuration A, which remained essentially constant (see figs. 6(c) to 11(c)). This increase in jet-thrust ratio is attributed to the increase in the momentum of the secondary air flow and to the restriction of the overexpansion of the primary jet by the secondary flow. Increasing the primary pressure ratio at a constant cooling-shroud pressure ratio had no effect on the jet-thrust ratio except for the ejector configurations having both large diameter and spacing ratios. The factors which influence the jet-thrust ratio for any ejector geometry, as the primary pressure ratio is increased, are: (1) there is less diffusion of the primary jet after reaching complete expansion in the ejector nozzle; (2) the momentum of the secondary air flow is increased by the smaller effective secondary air-flow passage and is decreased by the drop in secondary air flow; and (3) a probable decrease occurs in the mixing losses. In using the jet-thrust ratios, it should be kept in mind that the thrust with the ejector was not penalized in any way for the inlet momentum of the secondary air.

[redacted]

Effects of changes in ejector geometry. - For configuration A, which had a diameter ratio of 1.42 but about zero spacing ratio, changes in primary and cooling-shroud pressure ratios had no appreciable effect on the secondary pressure ratio. Increasing the spacing ratio for the same diameter ratio (configurations B and C (figs. 7(a) and 8(a)) decreased the secondary pressure ratio at a given cooling-shroud inlet and primary pressure ratio. This decrease in secondary pressure ratio resulted from greater friction pressure loss brought about by the higher secondary air flow through the cooling-shroud passage; the higher secondary air flow was induced by the increased pumping action of the primary jet as the spacing ratio was raised.

Changing the ejector diameter ratio from 1.42 to 1.08 resulted in reductions in secondary air flow, which in turn decreased the friction pressure drop in the cooling-shroud passage and caused an increase in the secondary pressure ratio (see configurations B and D, figs. 7(a) and 9(a), or C and E, figs. 8(a) and 10(a)). The increase in secondary pressure ratio became more pronounced at the higher primary pressure ratios.

For a diameter ratio of 1.42, increasing the spacing ratio at constant cooling-shroud inlet and primary pressure ratio raised the secondary air flow because of the greater pumping action of the primary jet. For example, at a cooling-shroud pressure ratio of 1.1 and a primary pressure ratio of 2.73, ejectors having a diameter ratio of 1.42 and spacing ratios of 0.04, 0.79, and 1.16 had gas-flow ratios of 0.030, 0.059, and 0.070, respectively (see figs. 6(b), 7(b), and 8(b)). However, at the high cooling-shroud pressure ratios, where a choking condition is approached in the cooling-shroud passage, changes in ejector spacing ratio had less effect on the pumping action of the primary jet. For the same change in spacing ratio at a primary pressure ratio of 2.73, the gas-flow ratio increased from 0.107 to 0.130 at a cooling-shroud pressure ratio of 1.6. For configurations having a diameter ratio of 1.08, a second effect exists which overrides the increased pumping action of the primary jet as the spacing ratio is increased with a net result of lowering the gas-flow ratio. This second effect is the increase in flow area of the primary jet at the exit of the ejector nozzle which results in a reduction of the flow passage for the secondary air stream.

An increase in primary pressure ratio, which increased the expansion of the primary jet, or a decrease in ejector diameter ratio both reduced the flow passage area for the secondary air. For an ejector having a diameter ratio of 1.08, in order to maintain a gas-flow ratio of 0.02 as the primary pressure ratio is raised from 1.79 to 3.40, the cooling-shroud inlet pressure ratio must be increased from 0.975 to 1.53 (see fig. 9(b)). At a cooling-shroud pressure ratio of 1.6, decreasing the ejector diameter ratio from 1.42 to 1.08 for a primary pressure ratio of 3.40 lowered the gas-flow ratio from 0.092 to 0.031 (see figs. 7(b) and 9(b)).

[redacted]

For a given primary pressure ratio, increasing the spacing ratio decreased the jet-thrust ratio because the increased losses due to diffusion of the primary jet and the greater mixing losses were larger than the increase in momentum and magnitude of the secondary air flow. At a diameter ratio of 1.42, a cooling-shroud inlet pressure ratio of 1.6, and a primary pressure ratio of 2.73, the jet-thrust ratios were 0.98, 0.94, and 0.89 for spacing ratios of 0.04, 0.79, and 1.16, respectively (see figs. 6(c), 7(c), and 8(c)). Changing the diameter ratio from 1.42 to 1.08 increased the jet-thrust ratio because of the large reduction in the overexpansion of the primary jet and small increase in momentum of secondary air flow. At a spacing ratio of 0.79, a cooling-shroud inlet pressure ratio of 1.6, and a primary pressure ratio of 2.73, the jet-thrust ratios were 0.94 and 1.005 for diameter ratios of 1.42 and 1.08, respectively (see figs. 7(c) and 9(c)).

Changes in primary exhaust-nozzle area were made for configurations A and D at primary pressure ratios of 2.73 and 3.40. It should be realized that these changes in primary nozzle area change the diameter and spacing ratios for each configuration. However, changing the primary nozzle area does represent a consideration in the practical application of ejectors on afterburner installations.

The performance of configurations A and D is shown in figures 12 and 13, respectively, for the three primary exhaust-nozzle areas - 266 (full open), 254, and 233 square inches. The performance variations of the ejector as the primary nozzle area is changed show the same trends as the performance variation for basic changes in ejector geometry. Decreasing the primary nozzle area results in an increase in ejector diameter ratio and a decrease in mixing length because the lips of the variable-area nozzle move downstream as the area is reduced. A reduction in primary nozzle area (increase in diameter ratio) permits a greater overexpansion of the primary jet, which results in a reduction in jet-thrust ratio, but permits a greater secondary air flow. However, for the primary nozzle-area change reported herein (diameter ratio increased from 1.08 to 1.152), there was little change in jet-thrust ratio. The higher secondary air flow is accompanied by a higher secondary air velocity, causing a greater pressure drop in the cooling shroud. For example, reducing the primary nozzle area from 266 to 233 square inches for configuration D resulted in a decrease in secondary pressure ratio from 1.37 to 1.17, an increase in gas flow from 0.082 to 0.104, and little effect on jet-thrust ratio at primary and cooling-shroud inlet pressure ratios of 2.73 and 1.60, respectively (fig. 13).

Effect of Gas-Flow Ratio on Primary Exhaust-Gas Temperature, Ejector Temperature Ratio, and Shell Temperature

Effect of gas-flow ratio on primary exhaust-gas temperature. - The variation of exhaust-gas temperature with gas-flow ratio at several

primary pressure ratios is shown in figure 14 for all the ejector configurations investigated. At high primary pressure ratios, changes in gas-flow ratio for the range investigated had no appreciable effect on the exhaust-gas temperature. At the lowest primary pressure ratio, however, increasing the gas-flow ratio tended to reduce the exhaust-gas temperature for ejectors with diameter ratios of 1.08, but there was little effect on the ejector with a diameter ratio of 1.42. This decrease in temperature results from the reduction in effective area of the primary jet by interference from the secondary air flow, requiring a reduction in the tail-pipe fuel flow in order to maintain constant turbine conditions.

Effect of gas-flow ratio on ejector temperature ratio. - The variation of ejector temperature ratio (defined as the ratio of primary exhaust-gas temperature to secondary air temperature measured at the inlet of the ejector nozzle) with gas-flow ratio is presented in figure 15. Figure 15(a) shows that primary pressure ratio has no effect on ejector temperature ratio, but increasing the gas-flow ratio decreases the secondary air temperature and thus raises the ejector temperature ratio. This relation was plotted for each ejector configuration, and the faired curves are shown in figure 15(b). For each ejector configuration, a given gas-flow ratio defines a single ejector temperature ratio, and within the range of gas-flow ratio investigated the temperature ratios varied from 2.0 to 5.0. At a given gas-flow ratio, the effect of changes in ejector geometry was relatively small because the secondary air temperature was measured at the cooling-shroud outlet passage, which is the entrance to the ejector nozzle (station d, fig. 3).

Effect of gas-flow ratio on afterburner shell temperatures. - The variation of afterburner shell temperatures with gas-flow ratio is presented in figure 16 for all ejector configurations. The afterburner shell temperature was measured at two stations: (1) just ahead of the afterburner flame holder (station c, fig. 3) and (2) at the inlet of the primary nozzle (station d, fig. 3). The primary gas temperatures ahead of the flame holder were essentially the turbine-outlet temperature (1660° R) for all operating conditions, and at the inlet to the primary nozzle, primary gas temperatures were about the same as the afterburner exhaust-gas temperature. Variations in primary pressure ratio had no effect on the shell temperatures (see fig. 16(a) for configuration B). The faired curves for each ejector configuration are presented in figure 16(b). From this figure it is apparent that a given gas-flow ratio defines approximately the same afterburner shell temperature for all the ejector configurations tested. An evaluation of the ejector cooling effectiveness should take into account that the afterburner was equipped with a cooling liner which extended the length of the combustion chamber (fig. 3).

Application of Ejector to Afterburner Installation

In the design of an afterburner ejector, two approaches might be considered: (1) the maintenance of constant afterburner shell temperature, and (2) constant ram pressure recovery at the cooling-shroud inlet. Because afterburner shell temperature is directly related to gas-flow ratio, performance plots are presented at constant gas-flow ratios. For the condition of constant pressure recovery, performance curves are presented for cooling-shroud inlet pressure ratios which correspond to values of constant engine-inlet pressure recovery at the cooling-shroud inlet. The range of primary pressure ratio investigated, which was from 1.79 to 3.40, corresponds to engine-inlet pressure ratios from 1.05 to 2.0, or flight Mach numbers from 0.25 to 1.08.

Ejector design for constant gas-flow ratio. - The variation of cooling-shroud inlet pressure ratio and jet-thrust ratio with primary pressure ratio is presented in figures 17 and 18, respectively, for constant gas-flow ratios of 0.04, 0.10, and 0.16 for all the ejector configurations investigated. A line which represents 100-percent recovery of engine-inlet pressure at the inlet of the cooling shroud has been superimposed on each of the shroud inlet pressure curves. Operation below this line might be possible with the use of ram air alone; however, operation above the line would require the use of high-pressure air from some auxiliary source.

Differences in ejector geometry have a large effect on the cooling-shroud inlet pressure required to maintain a constant gas-flow ratio (fig. 17). At a diameter ratio of 1.42, a gas-flow ratio of 0.04, and a primary pressure ratio of 3.04, increasing the spacing ratio from 0.04 to 1.16 lowered the cooling-shroud inlet pressure ratio from 1.18 to 0.89 (see configurations A and C, fig. 17(a)). At the same operating conditions for a spacing ratio of 0.79, decreasing the diameter ratio from 1.42 to 1.08 increased the shroud inlet pressure ratio, for constant gas-flow ratio, from 1.01 to 1.48 (see configurations B and D, fig. 17(a)). As the cooling-air flows are increased, however, the effects of ejector geometry on cooling-shroud inlet pressure ratio are diminished (see figs. 17(b) and 17(c)).

An important consideration in the selection of the most suitable ejector geometry for the maintenance of constant gas-flow ratio (constant shell temperature) is the relative position of the performance curves with respect to the 100-percent ram pressure recovery line. The cooling-shroud inlet pressure required to maintain low gas-flow ratios is considerably less than the pressure available at the engine inlet (see fig. 17(a)). As the gas-flow ratio is increased, however, the pressure required at the inlet to the cooling shroud becomes greater than the pressure available at the engine inlet and thus would require an auxiliary supply of high-pressure air.

The variation of jet-thrust ratio with primary pressure ratio for gas-flow ratios of 0.04, 0.10, and 0.16 is presented in figures 18(a), 18(b), and 18(c), respectively, for all ejector configurations. At a diameter ratio of 1.42, increasing the spacing ratio from 0.04 to 1.16 resulted in reductions in jet-thrust ratio as high as 15 percent. However, changing the spacing ratio for a diameter ratio of 1.08 had a much smaller effect on the jet-thrust ratio. Lowering the diameter ratio from 1.42 to 1.08 resulted in thrust increases of about 8 and 12 percent for spacing ratios of 0.79 and 1.16, respectively (see figs. 18(a), 18(b), and 18(c)).

Ejector design for constant engine-inlet ram pressure recovery. - The variation of gas-flow ratio and jet-thrust ratio with primary pressure ratio is presented in figures 19 and 20, respectively, for constant pressures at the cooling-shroud inlet of 100, 70, and 40 percent of the ram pressure available at the engine inlet. At a given ram pressure recovery, the ejectors with larger diameter ratios permitted a substantially greater gas-flow ratio to be obtained at any primary pressure ratio (fig. 19). For example, at a ram pressure recovery of 100 percent, a primary pressure ratio of 2.73, and a spacing ratio of 0.79, raising the diameter ratio from 1.08 to 1.42 increased the gas-flow ratio from 0.082 to 0.116. For ejector configuration C, reducing the ram pressure recovery from 100 to 40 percent lowered the gas-flow ratio from 0.126 to 0.088 at a primary pressure ratio of 2.73. The effects of variations in ejector geometry on the jet-thrust ratio at constant ram pressure recovery (fig. 20) are similar to those indicated for constant gas-flow ratio (fig. 18).

Design criterion for optimum performance. - In the selection of an optimum ejector design, a compromise must be reached by weighing the following factors: (1) the secondary air flow required to keep the afterburner skin temperature within allowable limits, (2) the pressure that would be available at the inlet to the cooling shroud, and (3) the thrust loss at critical flight conditions. From figures 17 to 20, it is possible to develop a qualitative idea of the effect of ejector geometry on the gas-flow ratio, the cooling-shroud pressure requirements, and the jet-thrust penalties. An examination of these curves leads to the following general conclusions:

(1) For ejectors with large diameter ratios, reasonable gas-flow ratios can be obtained at relatively low pressures at the entrance to the cooling shroud, but the thrust losses become prohibitive as the spacing ratio is increased from 0 to 1.16.

(2) For ejectors with small diameter ratios, reasonable gas-flow ratios can be obtained only at high cooling-shroud inlet pressures; however, the thrust characteristics are superior to those obtained for ejectors with large diameter ratios. At high flight Mach numbers, use of the small-diameter-ratio ejectors may permit the attainment of a jet-thrust gain.

[redacted]

(3) From the data presented, it is evident that a particular ejector configuration for a flight installation will depend on the specific design requirements. However, results of the present ejector investigation show that maximum air-flow and thrust characteristics cannot be obtained from any one ejector geometry, but that compromises must be made of one for the other.

Investigation of Effect of Temperature Ratio on Corrected Ejector Performance

A comparison of test data obtained from two independent sources (references 1 and 2) is presented in figure 21 for similar ejector geometries and for equal primary and secondary air temperatures. This comparison is made with gas-flow ratio as a function of primary pressure ratio for two secondary pressure ratios. Because the data from both sources show good agreement even though the primary nozzle diameters were 0.78 and 4.0 inches for references 1 and 2, respectively, it appears that there are no scale effects.

When the temperatures of the secondary and primary air streams are not equal, the square root of the temperature ratio is suggested as a generalization factor for the gas-flow ratio in references 3 and 6. An investigation to determine the validity of this temperature-correction factor on the generalization of the gas-flow ratio is reported in reference 4. Data that indicate the effect of temperature ratio on the corrected gas-flow ratio for a hypothetical and an experimental ejector configuration are reproduced from reference 4 in figure 22. Increasing the temperature ratio from 1.0 to 3.0 at a primary pressure ratio of 1.6 decreased the corrected mass-flow ratio about 25 and 18 percent for the hypothetical and experimental ejectors, respectively, at secondary pressure ratios of 1.00, 1.05, and 1.10. It is therefore apparent that for the range covered in this investigation changes in temperature ratio between the primary and secondary air flows have a first-order effect on the corrected gas-flow ratio.

The data obtained in the full-scale altitude-wind-tunnel ejector investigation at temperature ratios from 2.0 to 5.0 are compared in figure 23 with model data from reference 2 for the same ejector geometry with a temperature ratio of 1.0. At given primary and secondary pressure ratios, the corrected gas-flow ratios indicated by the small-scale ejector data at a temperature ratio of 1.0 were much larger than those indicated by the full-scale ejector data obtained in the altitude-wind-tunnel investigation at temperature ratios from 2 to 5. For example, at a primary pressure ratio of 1.8 and a secondary pressure ratio of 1.05, the corrected gas-flow ratio for the hot, full-scale data is about 55 percent of the amount indicated by the cold model data. However, at higher primary pressure ratios the percentage difference between hot and cold ejector data increases.

[redacted]

Reference 6 indicates that a small variation in static pressure of the secondary air between conditions of different ejector temperature ratios will produce substantial changes in the corrected gas-flow ratio. For an example shown in the reference report where the secondary total pressure was the same but the secondary static pressure differed by about 0.2 of 1 percent, for hot and cold data, an error of 35 percent was obtained for the corrected gas-flow ratios. Therefore it seems likely that differences in secondary static pressure between hot and cold ejector data constitute a factor that prevents the generalization of gas-flow ratios by the simple temperature-correction factor.

From these comparisons it is apparent that ejector performance data obtained at a temperature ratio of 1.0 cannot be extrapolated to the temperature ratios required of turbojet afterburning operation by the simple temperature correction factor suggested in references 3 and 6.

SUMMARY OF RESULTS

The following results were obtained from a full-scale turbojet engine - afterburner installation equipped with a cooling shroud and a series of ejector nozzles:

1. For ejectors with large diameter ratios, reasonable gas-flow ratios could be obtained at relatively low pressures at the entrance to the cooling shroud, but the thrust losses became very large as the spacing ratio was increased from 0 to 1.16.

2. For ejectors with small diameter ratios, reasonable gas-flow ratios could be obtained only at high cooling-shroud inlet pressures; however, the thrust characteristics were superior to those obtained for ejectors with large diameter ratios. At high flight Mach numbers, use of the small-diameter ratio ejectors may permit the attainment of a small thrust gain over a simple convergent nozzle.

3. Changes in the variable-area exhaust nozzle (primary system) had the same effect on ejector performance as the corresponding changes of ejector diameter and spacing ratios with constant primary nozzle area.

4. For a given gas-flow ratio, a single ejector temperature ratio and afterburner shell temperature were obtained for all ejector nozzles investigated.

[redacted]

5. The full-scale altitude-wind-tunnel investigation of ejectors verified results previously reported - that secondary air-flow data obtained at a temperature ratio of 1.0 could not be extrapolated to determine air flow at temperature ratios between 2.0 and 5.0 by the application of the temperature-ratio factor to the gas-flow ratios.

Lewis Flight Propulsion Laboratory
National Advisory Committee for Aeronautics
Cleveland, Ohio

[redacted]

APPENDIX - CALCULATIONS

Symbols

A	cross sectional area, sq ft
B	thrust-scale balance force, lb
C_j	jet-thrust coefficient, ratio of scale jet thrust to rake jet thrust (without ejector)
C_F	flow coefficient
C_T	thermoexpansion coefficient, ratio of hot exhaust-nozzle area to cold exhaust-nozzle area
D	diameter, ft
D_i	external drag of installation, lb
F	jet thrust, lb
g	acceleration due to gravity, 32.2 ft/sec^2
L	mixing length, ft
P	total pressure, lb/sq ft absolute
p	static pressure, lb/sq ft absolute
q	impact pressure (P-p), lb/sq ft absolute
R	gas constant, 53.4 ft-lb/(lb)($^\circ$R)
S	distance from primary nozzle exit to ejector nozzle-section exit
T	total temperature, $^\circ$R
T_w	metal temperature, $^\circ$F
t	static temperature, $^\circ$R
V	velocity, ft/sec
W_a	air flow, lb/sec
W_f	fuel flow, lb/hr

W_p primary gas flow, lb/sec

W_s secondary air flow, lb/sec

γ ratio of specific heats of gases

Subscript:

e engine

Primary instrumentation stations:

r exhaust-nozzle survey rake

t tail-pipe

0 free-stream

1 inlet air duct

p primary exhaust nozzle outlet, 1 inch upstream of exhaust-nozzle fixed portion outlet

Secondary instrumentation stations:

A venturi in secondary air supply line upstream of plenum chamber

b plenum chamber

c cooling-shroud inlet

d cooling-shroud outlet

s secondary ejector-nozzle inlet

Parameters:

D_s/D_p ejector diameter ratio

S/D_p ejector spacing ratio

P_p/p_0 primary pressure ratio

P_s/p_0 secondary pressure ratio

W_s/W_p ejector gas-flow ratio

T_p/T_s ejector temperature ratio

[redacted]

Methods of Calculation

Primary gas flow. - Air flow at the engine inlet was determined from pressure and temperature measurements obtained in the inlet air duct by the equation

$$W_{a,1} = p_1 A_1 \sqrt{\frac{2\gamma_1 g}{(\gamma_1 - 1)Rt_1}\left[\left(\frac{P_1}{p_1}\right)^{\frac{\gamma_1 - 1}{\gamma_1}} - 1\right]}$$

Primary gas flow in the tail-pipe is

$$W_p = W_{a,1} + \frac{W_{f,e} + W_{f,t}}{3600}$$

Secondary air flow. - The secondary air flow was measured at the venturi located upstream of the shroud-inlet plenum chamber. Because the velocity of the air was low at this station, the following incompressible equation was used:

$$W_s = W_{a,A} = A_A \sqrt{\frac{2g}{R}} \sqrt{\frac{p_A q_A}{t_A}}$$

Primary exhaust-gas temperature. - The total temperature of the primary exhaust gas was determined from exhaust-nozzle total and static pressure and tail-pipe gas flow as follows:

$$T_p = \left(\frac{p_p C_F C_T A_p}{W_p}\right)^2 \left\{\frac{2\gamma_p}{(\gamma_p - 1)} \frac{g}{R}\left[\left(\frac{P_p}{p_p}\right)^{\frac{\gamma_p - 1}{\gamma_p}} - 1\right]\right\} \left(\frac{P_p}{p_p}\right)^{\frac{\gamma_p - 1}{\gamma_p}}$$

Jet thrust of combined primary and secondary systems. - The combined jet thrust was determined from the balance-scale measurements by the following equation:

$$F_{p+s} = B + D_i + D_r + \frac{W_{a,1} V_1}{g} + A_1(p_1 - p_0)$$

The last two terms represent momentum and pressure forces, respectively, acting on the installation at the slip joint in the inlet air duct. The

external drag of the installation was determined from experiments obtained with a blind flange installed at the engine inlet to prevent air flow through the engine.

Jet thrust of primary system. - The jet thrust of the primary system was calculated from exhaust-nozzle outlet pressures and tail-pipe gas flow obtained simultaneously with the combined jet thrust of the primary and secondary systems.

$$F_p = C_j\left[\frac{W_p}{g} V_n + A_n(p_n - p_0)\right]$$

where the subscript n denotes the station at the primary nozzle vena contracta and the jet thrust coefficient C_j determined from previous engine operation was 0.97. The charts in reference 7 were used in the solution of the preceding equations.

REFERENCES

1. Timbie, T. R.: Additional Data on the Use of Ejectors at the Jet Nozzle to Improve Cooling of Gas Turbine Installations. DF81425, Aircraft Gas Turbine Eng. Div., Gen. Elec. Co., Sept. 1945.

2. Huddleston, S. C., Wilsted, H. D., and Ellis, C. W.: Performance of Several Air Ejectors with Conical Mixing Sections and Small Secondary Flow Rates. NACA RM E8D23, 1948.

3. Kochendorfer, Fred D., and Rousso, Morris D.: Performance Characteristics of Aircraft Cooling Ejectors having Short Cylindrical Shrouds. NACA RM E51E01, 1951.

4. Mickey, F. E.: An Investigation of the Pumping and Thrust Characteristics of a Jet Ejector Operating at High Temperature & Pressure. Rep. ES 21468, Douglas Aircraft Company, Inc. (El Segundo, Calif.), June 24, 1949. (Contract NOa(s) 9517, Phase XI of W.O. 606.)

5. Morrisson, Reeves: Jet Ejectors and Augmentation. NACA ACR, Sept. 1942.

6. Wilsted, H. D., Huddleston, S. C., and Ellis, C. W.: Effect of Temperature on Performance of Several Ejector Configurations. NACA RM E9E16, 1949.

7. Turner, L. Richard, Addie, Albert N., and Zimmerman, Richard H.: Charts for the Analysis of One-Dimensional Steady Compressible Flow. NACA TN 1419, 1948.

[redacted]

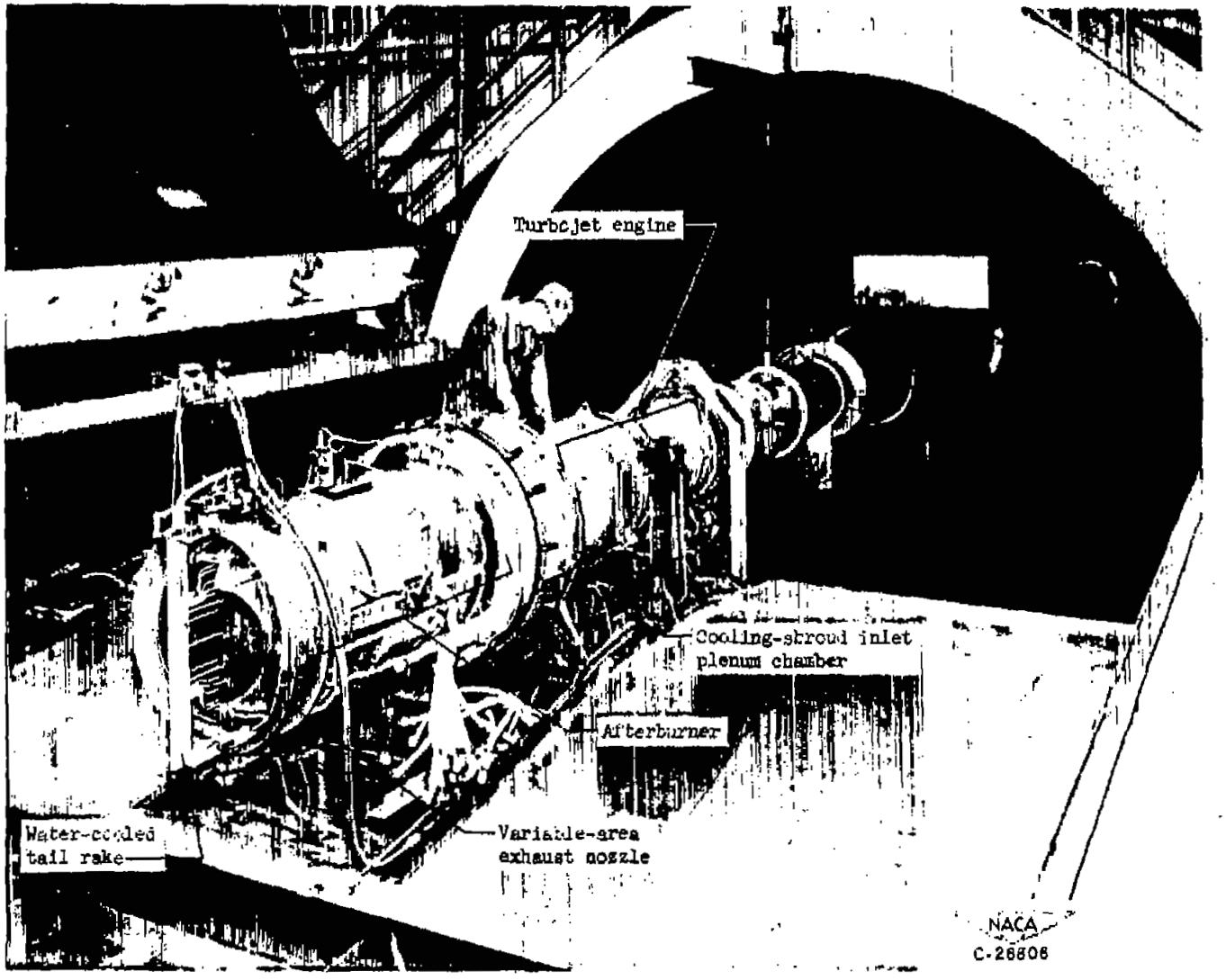

Figure 1. - Turbojet-afterburner engine installation in altitude wind tunnel with cooling shroud installed.

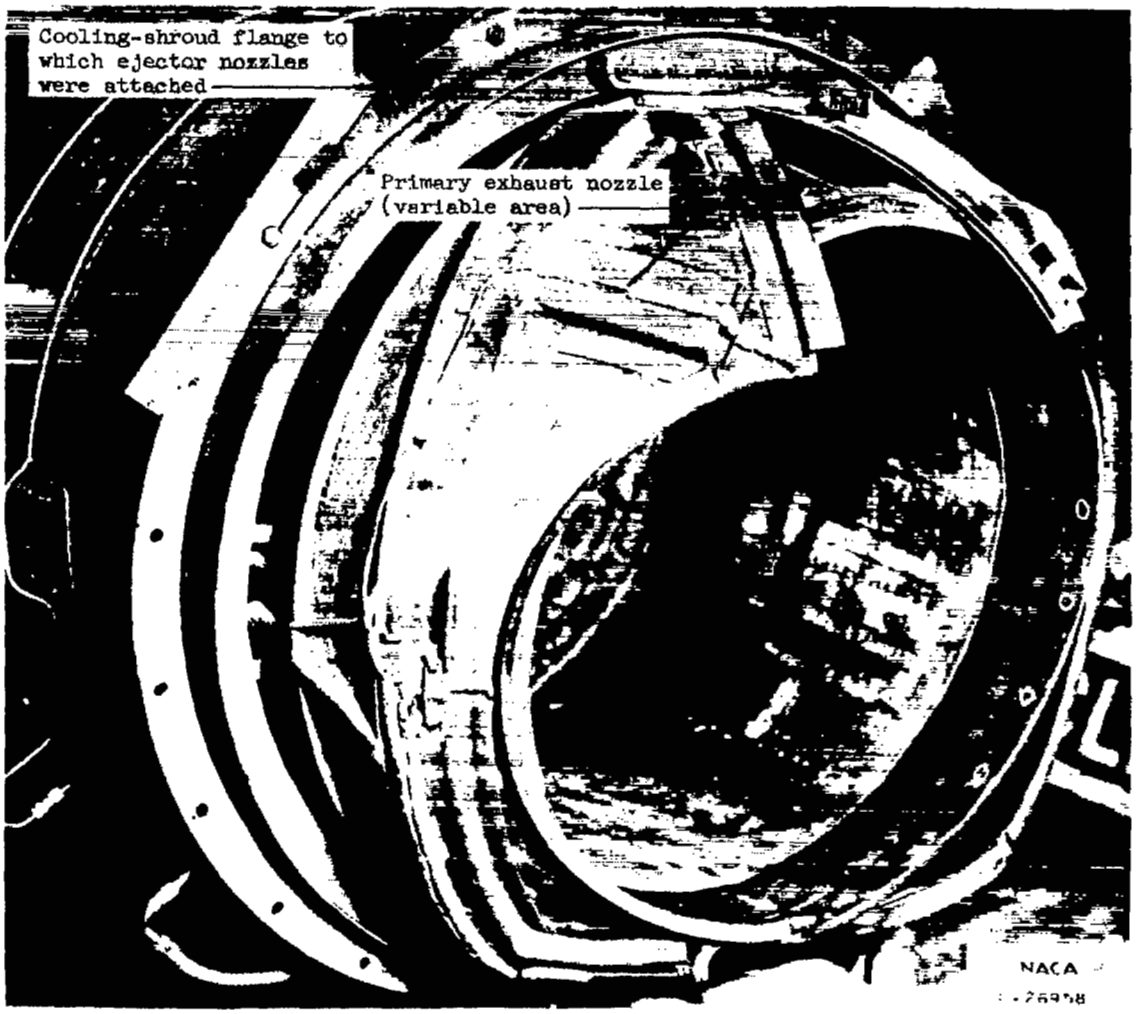

Figure 2. - View of afterburner cooling shroud and primary exhaust nozzle.

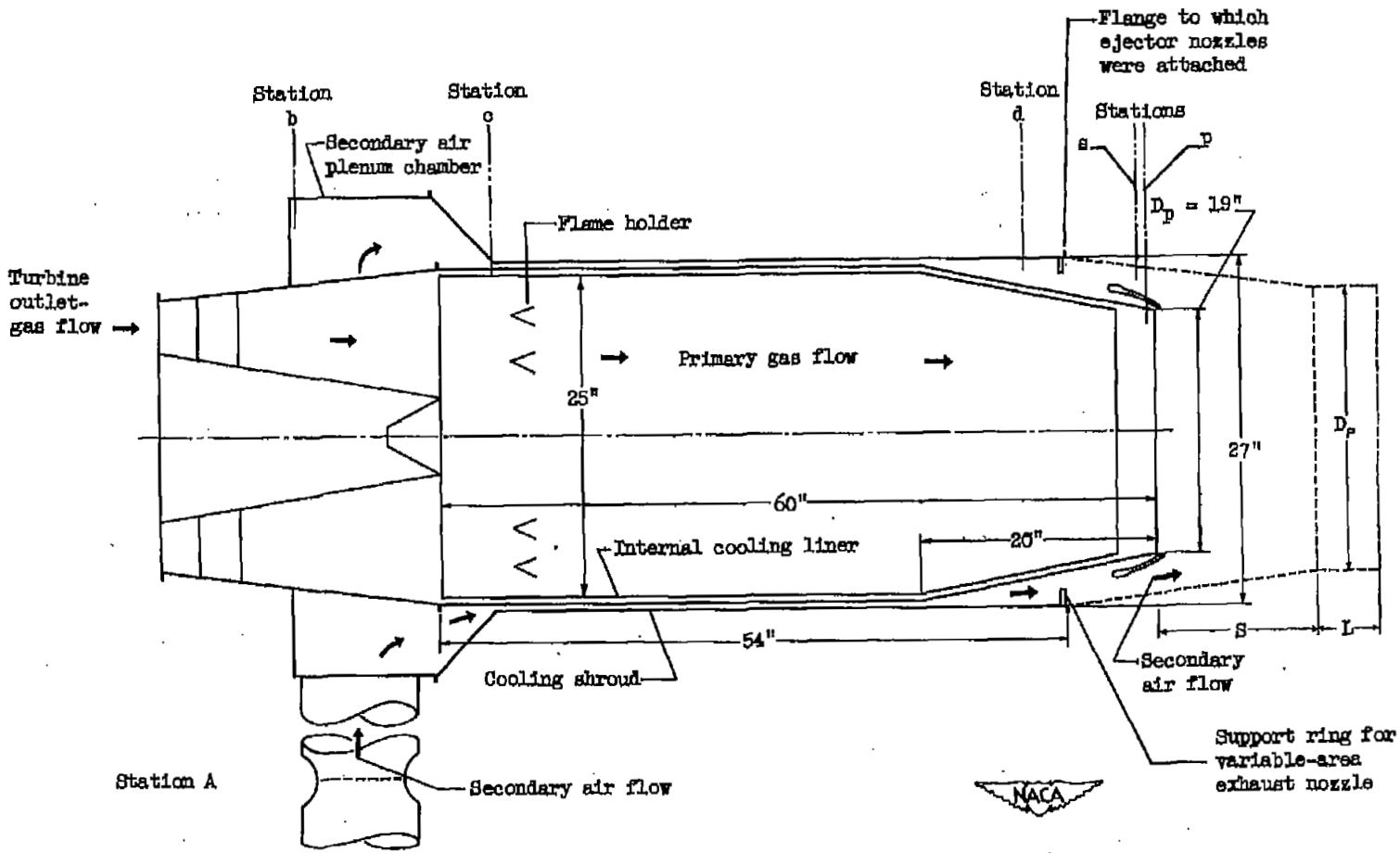

Figure 3. - Sketch of afterburner showing secondary and primary gas-flow passages.

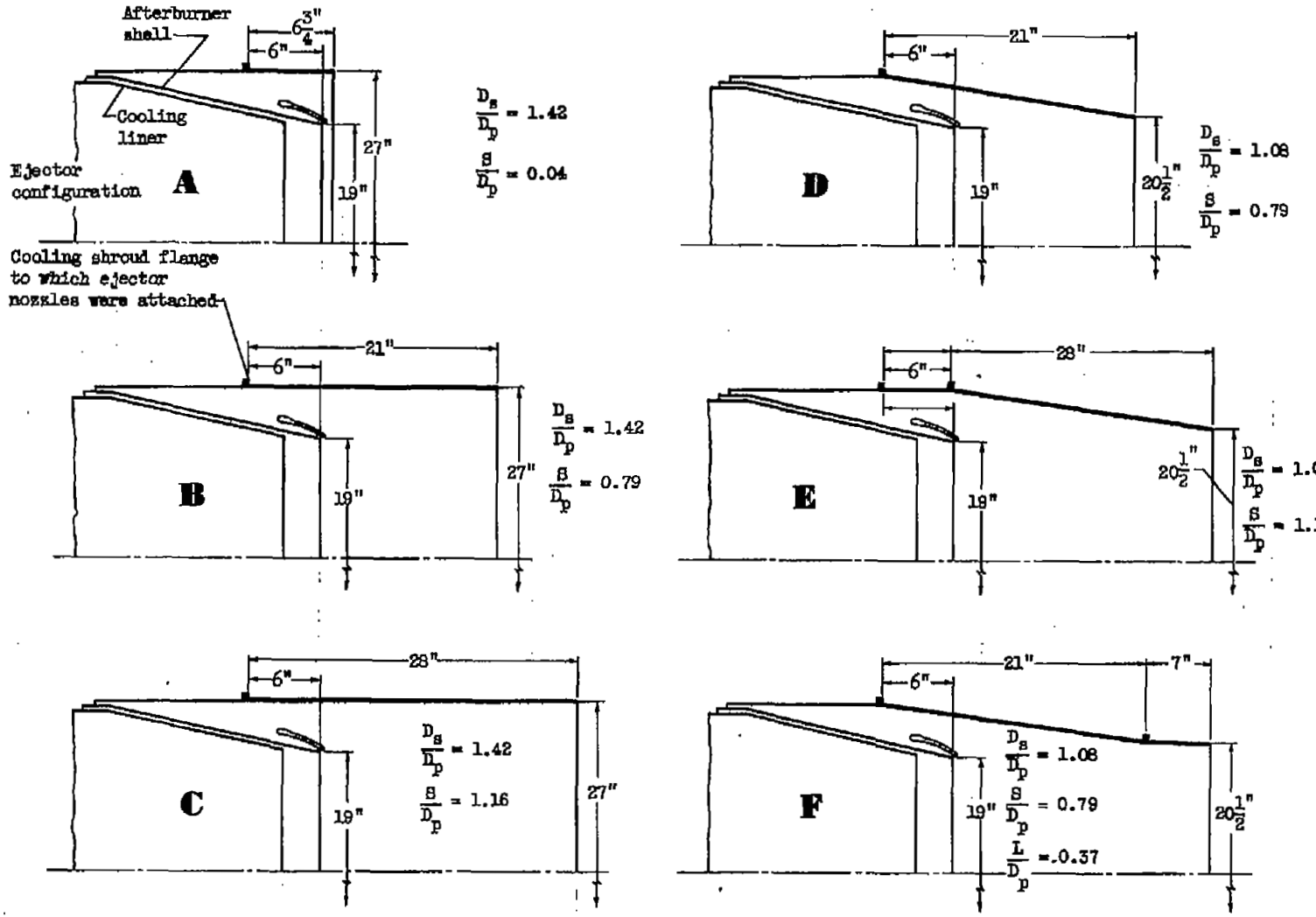

Figure 4. - Sketch of ejector configurations used in altitude wind tunnel full-scale ejector study.

NACA

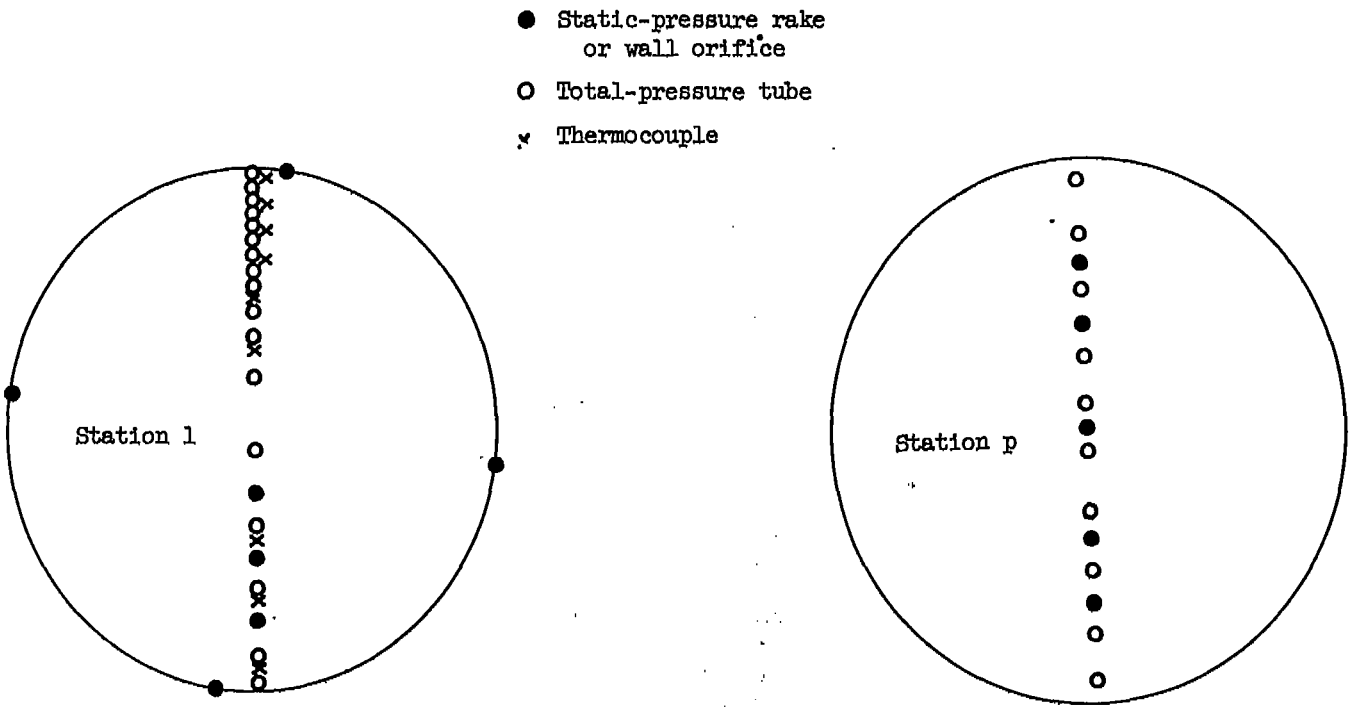

(a) Primary measuring stations.

Figure 5. - Cross sections showing location of instrumentation.

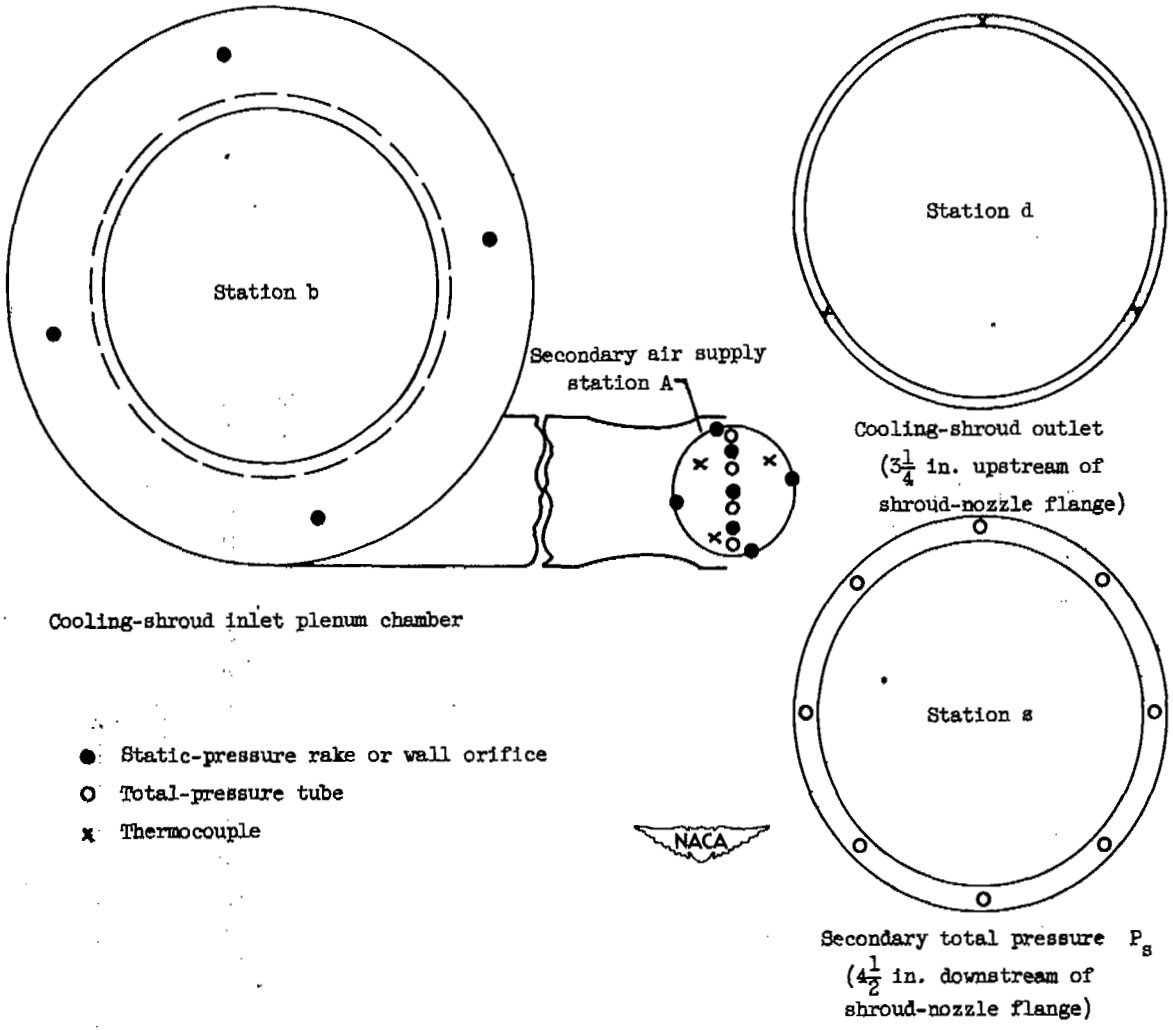

(b) Secondary measuring stations.

Figure 5. - Concluded. Cross sections showing location of instrumentation.

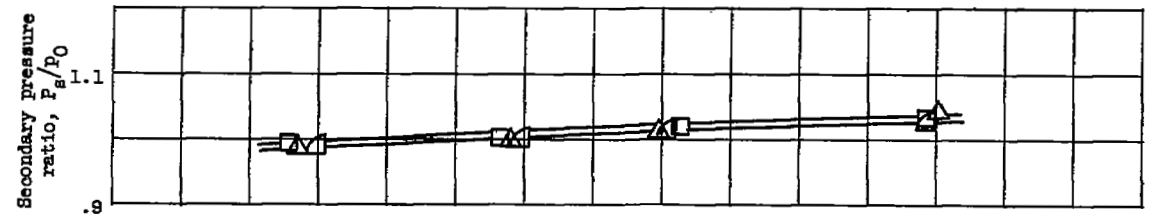

(a) Secondary pressure ratio.

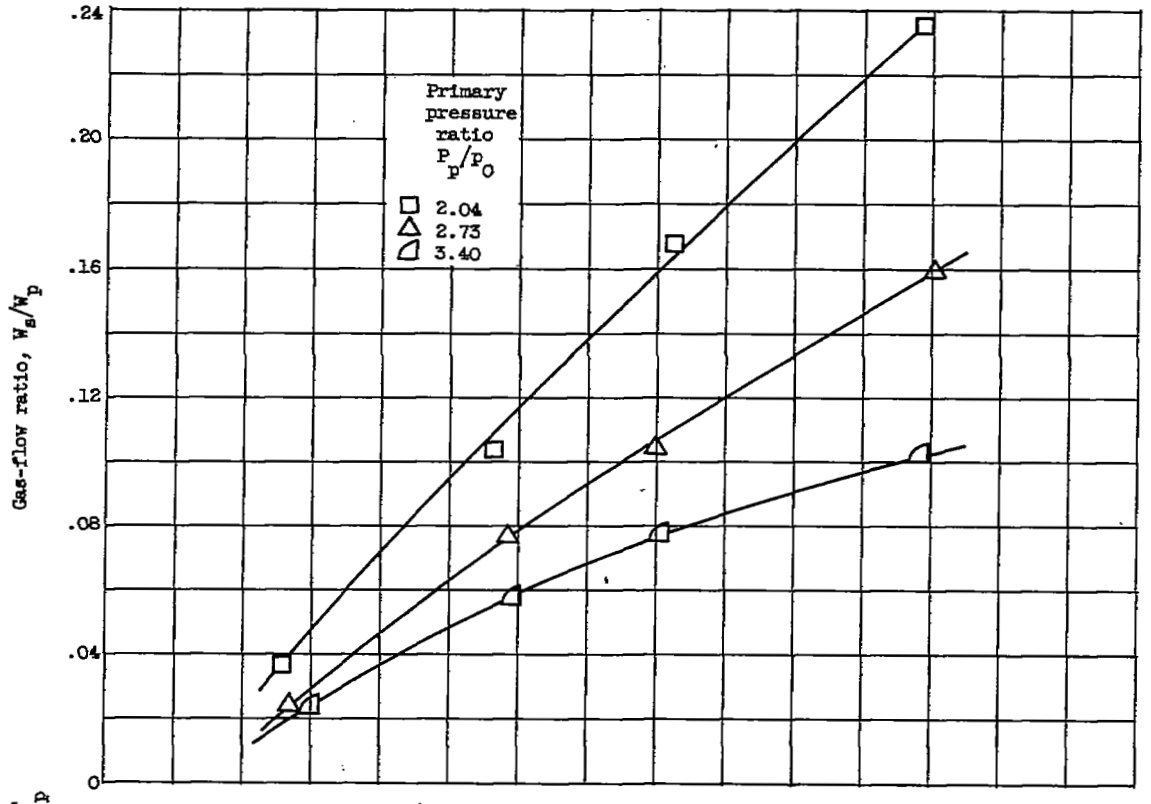

(b) Gas-flow ratio.

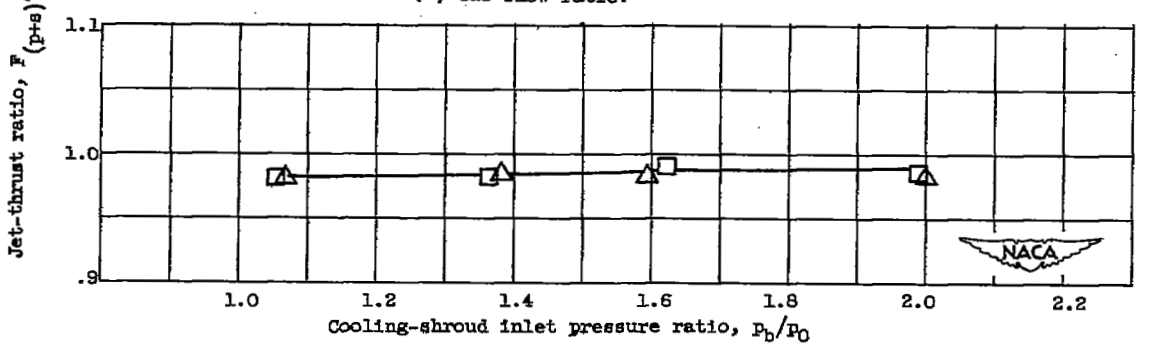

(c) Jet-thrust ratio.

Figure 6. - Variation of ejector performance parameters with cooling-shroud inlet pressure ratio for configuration A.

[redacted]

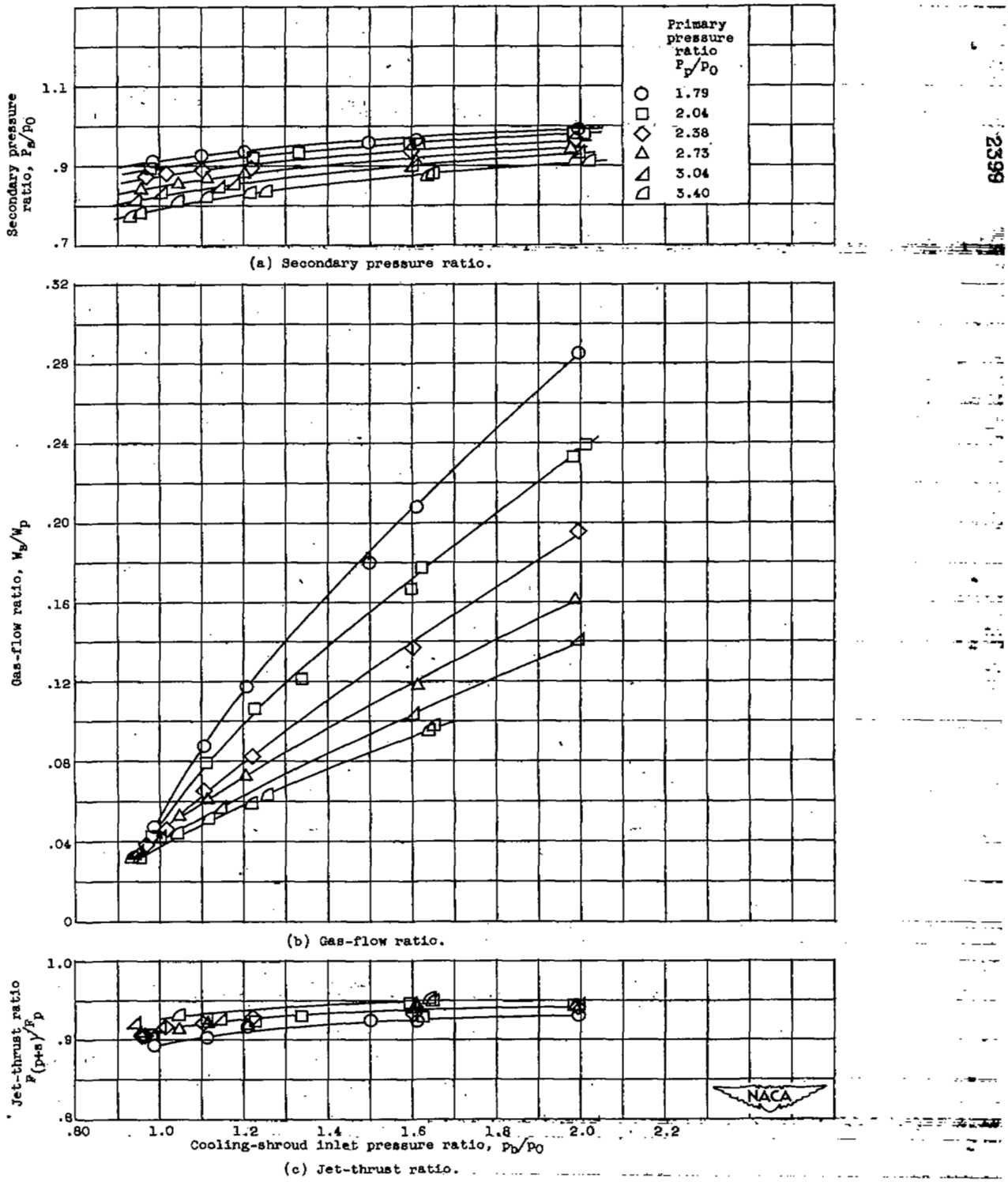

Figure 7. - Variation of ejector performance parameters with cooling-shroud inlet pressure ratio for configuration B.

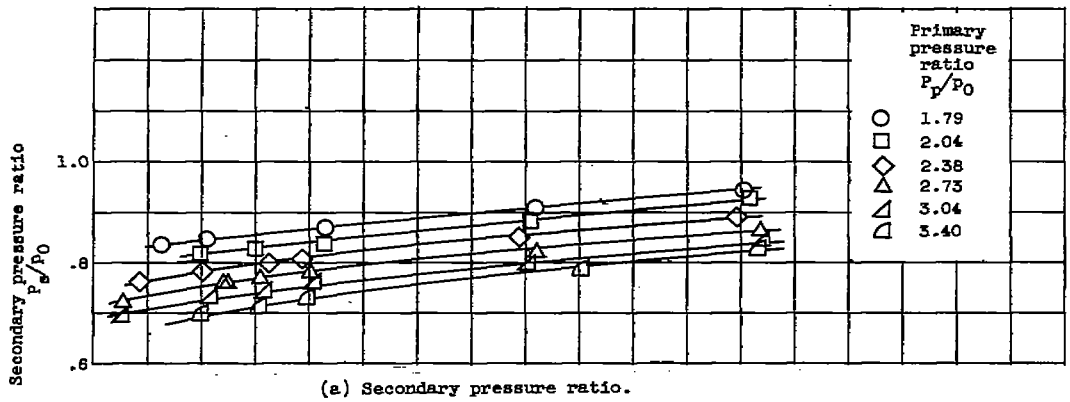

(a) Secondary pressure ratio.

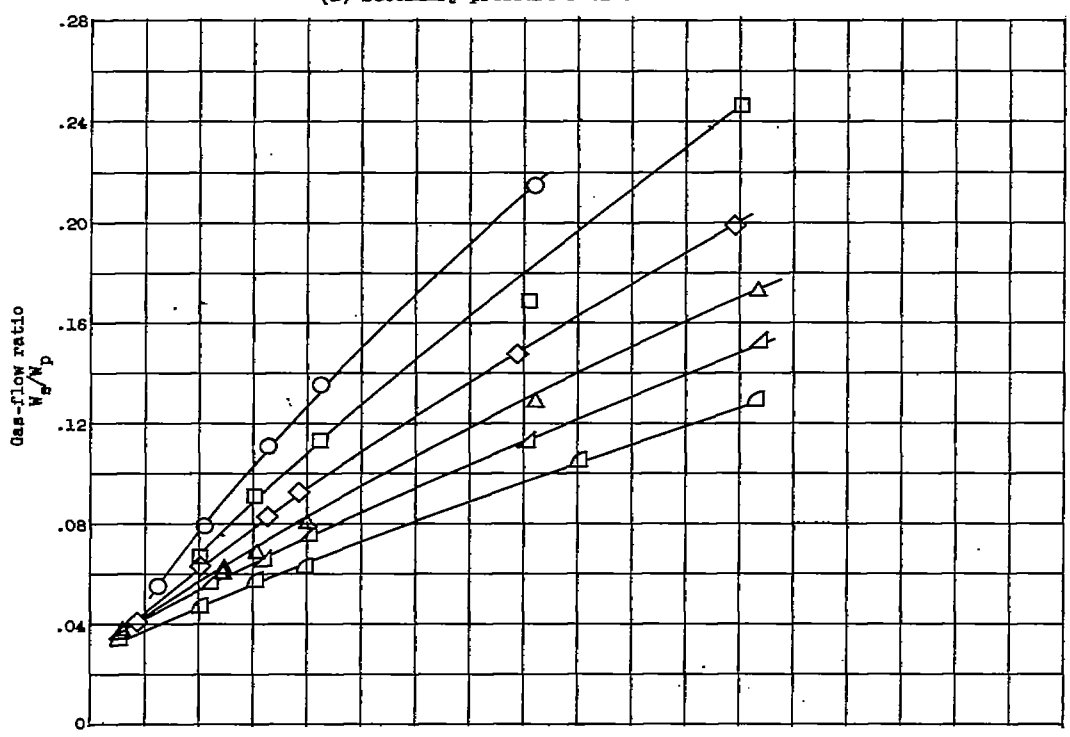

(b) Gas-flow ratio.

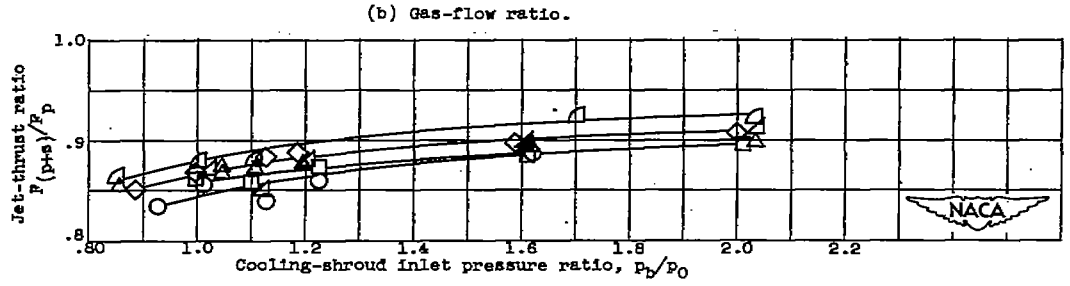

(c) Jet-thrust ratio.

Figure 8. - Variation of ejector performance parameters with cooling-shroud inlet pressure ratio for configuration C.

[redacted]

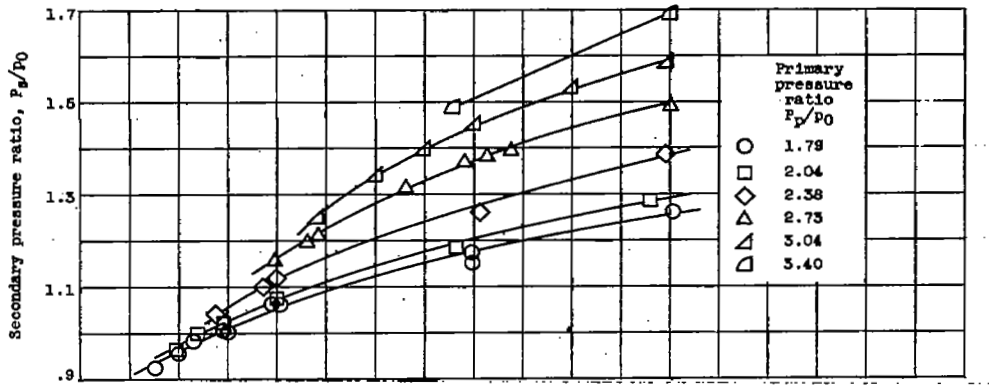

(a) Secondary pressure ratio.

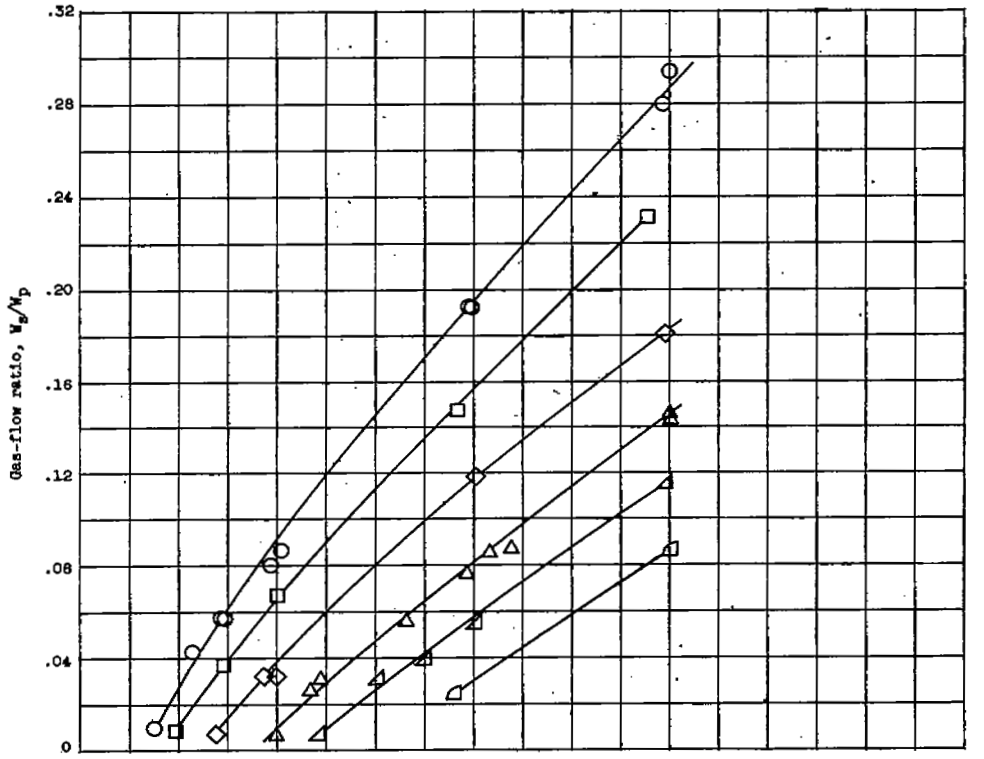

(b) Gas-flow ratio.

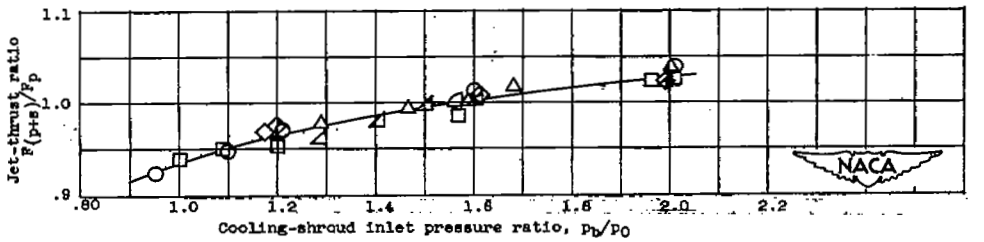

(c) Jet-thrust ratio.

Figure 9. - Variation of ejector performance parameters with cooling-shroud inlet pressure ratio for configuration D.

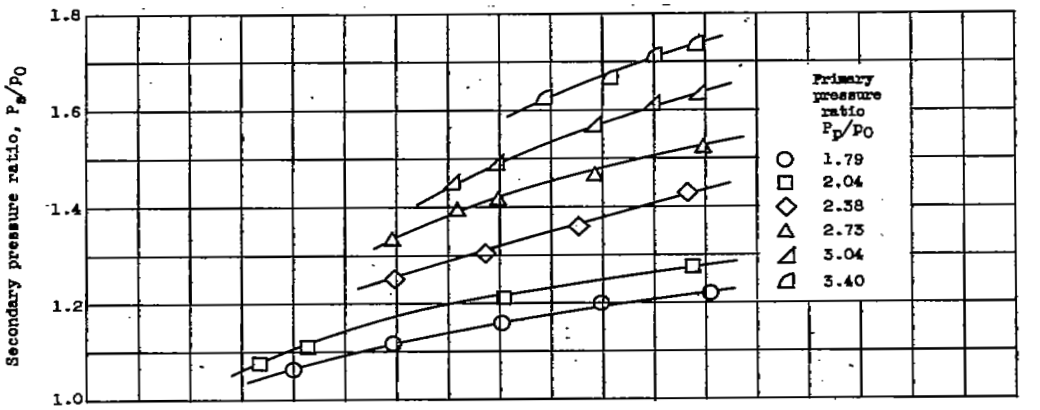

(a) Secondary pressure ratio.

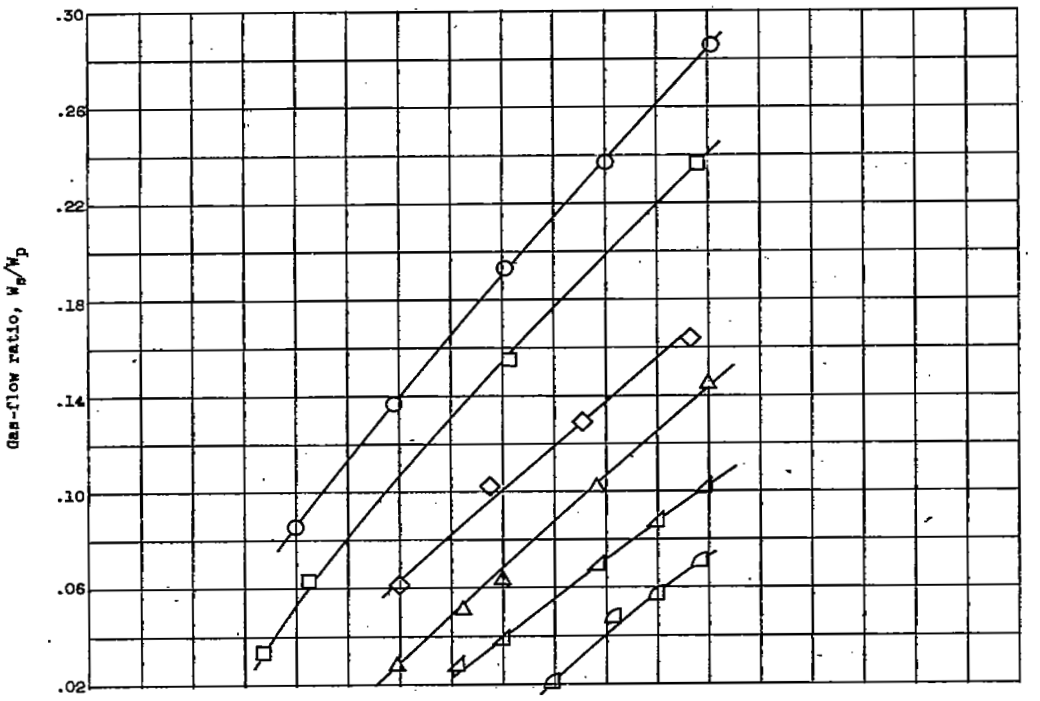

(b) Gas-flow ratio.

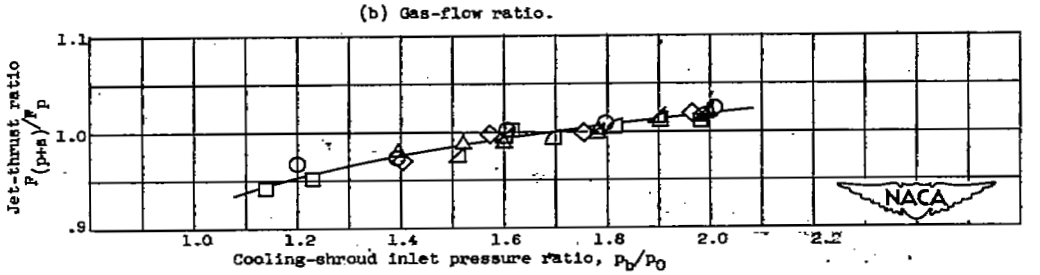

(c) Jet-thrust ratio.

Figure 10. - Variation of ejector performance parameters with cooling-shroud inlet pressure ratio for configuration E.

[redacted]

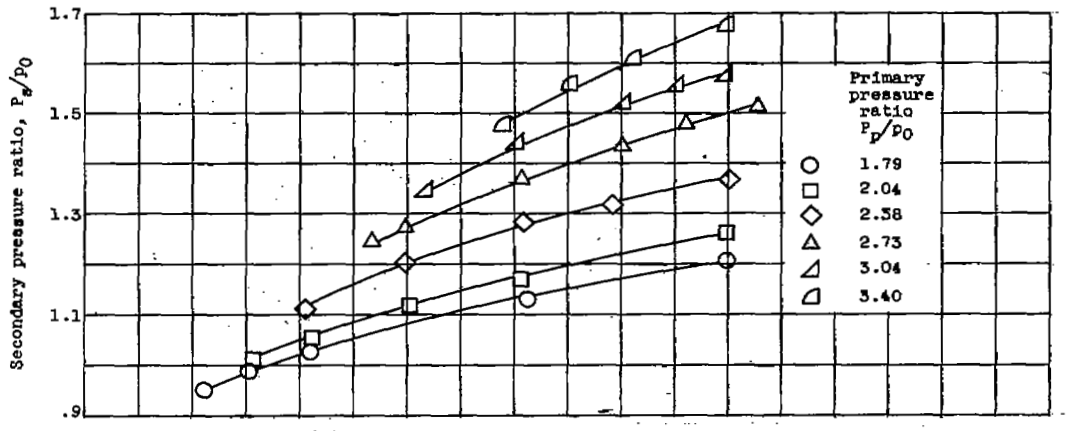

(a) Secondary pressure ratio.

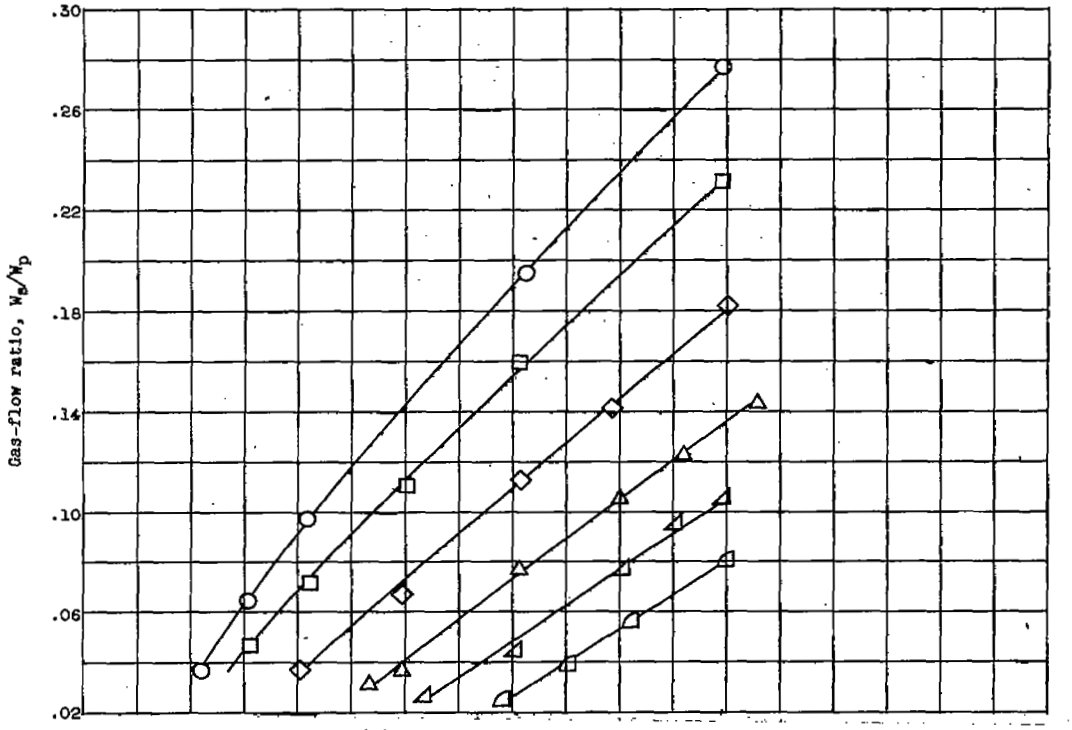

(b) Gas-flow ratio.

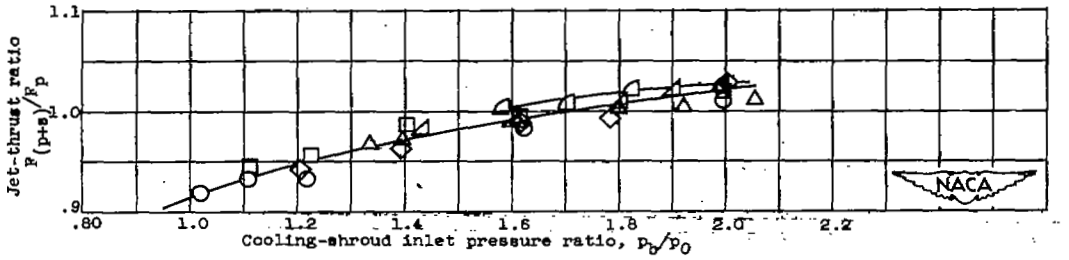

(c) Jet-thrust ratio.

Figure 11. - Variation of ejector performance parameters with cooling-shroud inlet pressure ratio for configuration F.

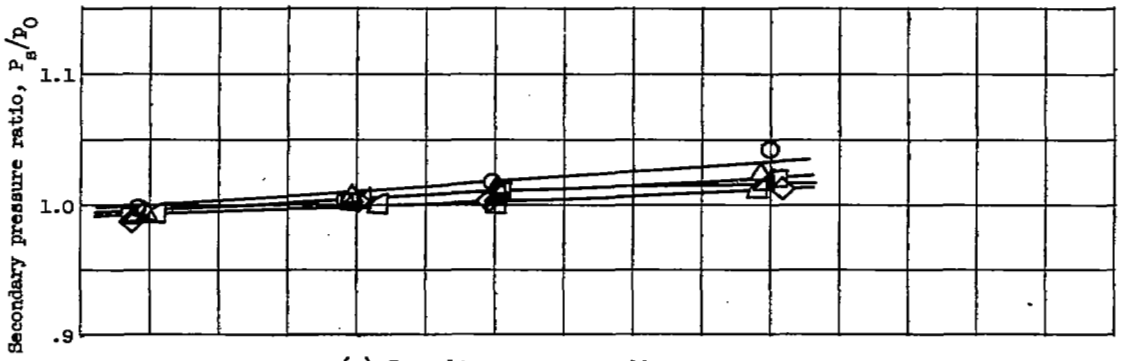

(a) Secondary pressure ratio.

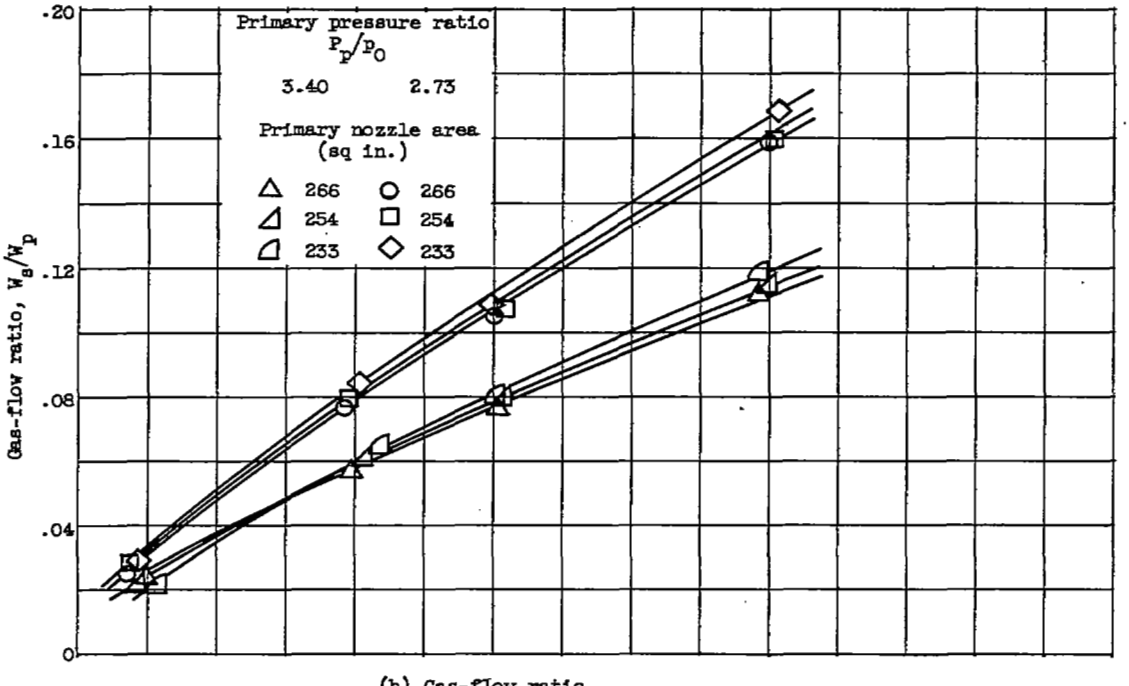

(b) Gas-flow ratio.

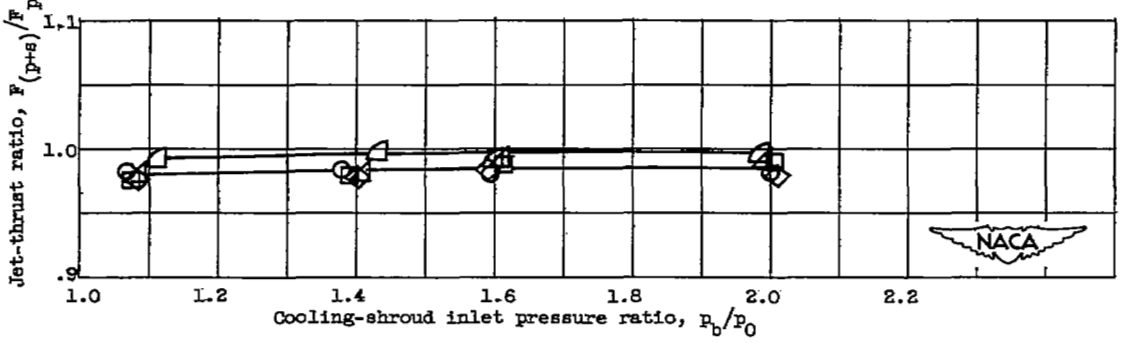

(c) Jet-thrust ratio.

Figure 12. - Effect of changes in primary nozzle area on variation of ejector performance parameters with cooling-shroud inlet pressure ratio for configuration A.

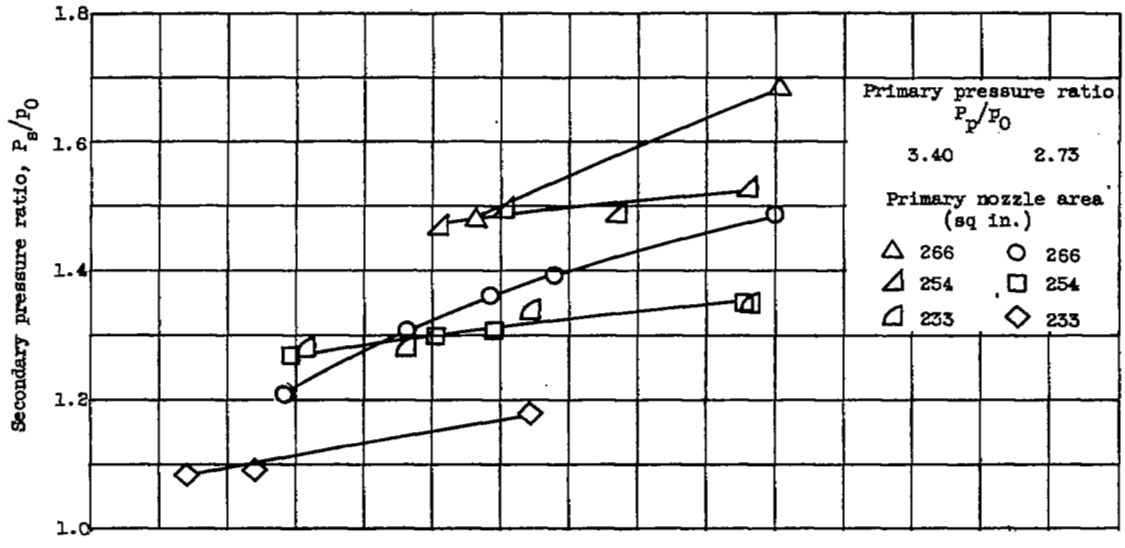

(a) Secondary pressure ratio.

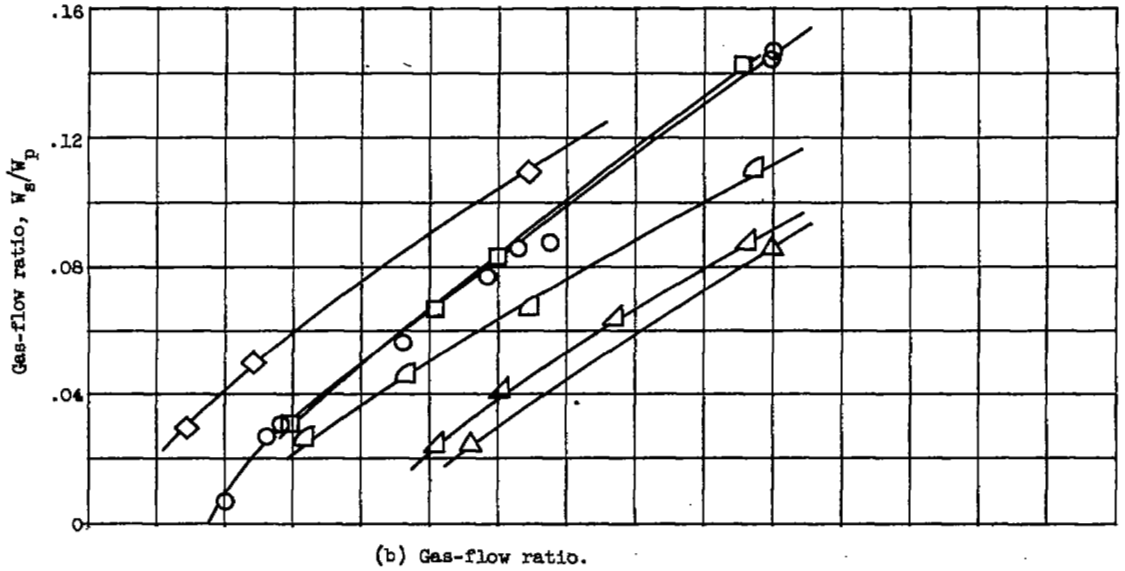

(b) Gas-flow ratio.

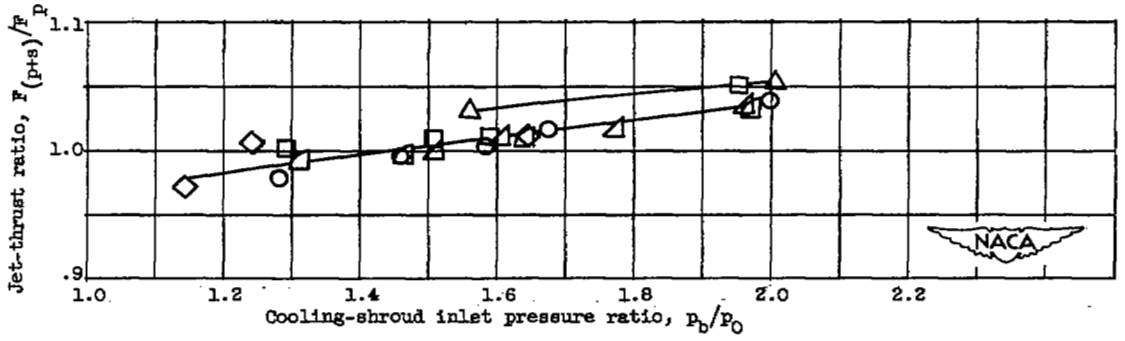

(c) Jet-thrust ratio.

Figure 13. - Effect of changes in primary nozzle area on variation of ejector performance parameters with cooling-shroud inlet pressure ratio for configuration D.

[redacted]

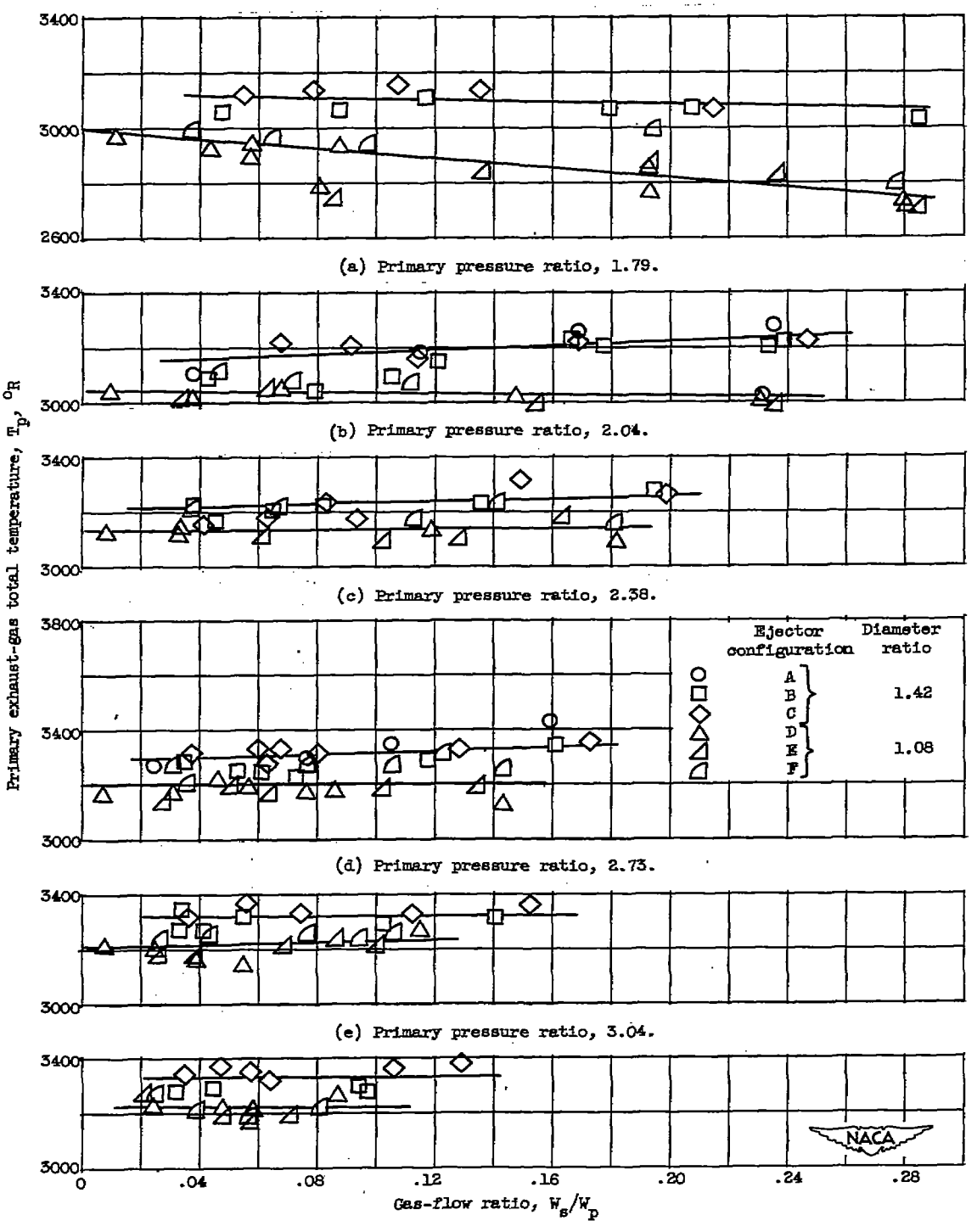

Figure 14. - Variation of primary exhaust-gas temperature with gas-flow ratio for all configurations.

[redacted]

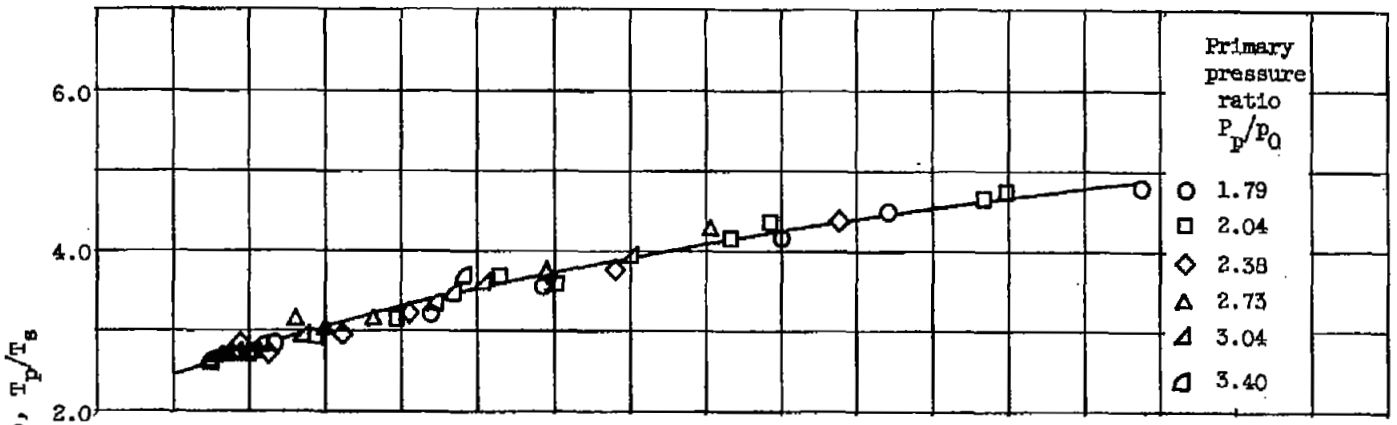

(a) Variation of temperature ratio for configuration B.

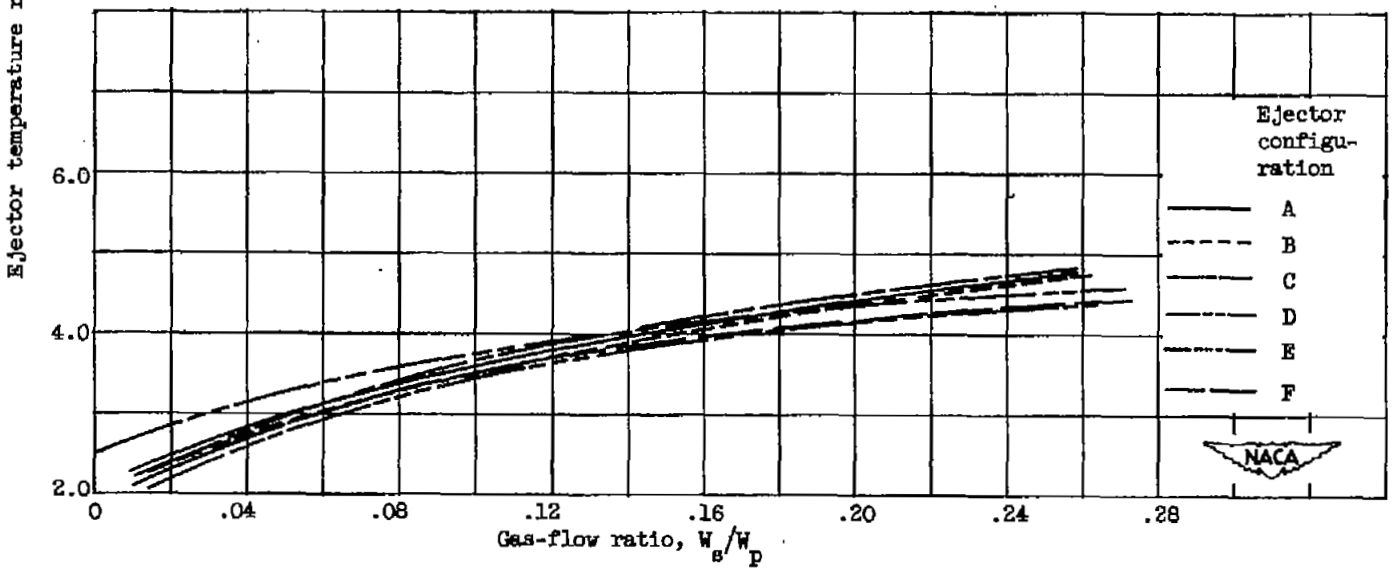

(b) Variation of temperature ratio for all configurations.

Figure 15. - Variation of ejector temperature ratio with gas-flow ratio.

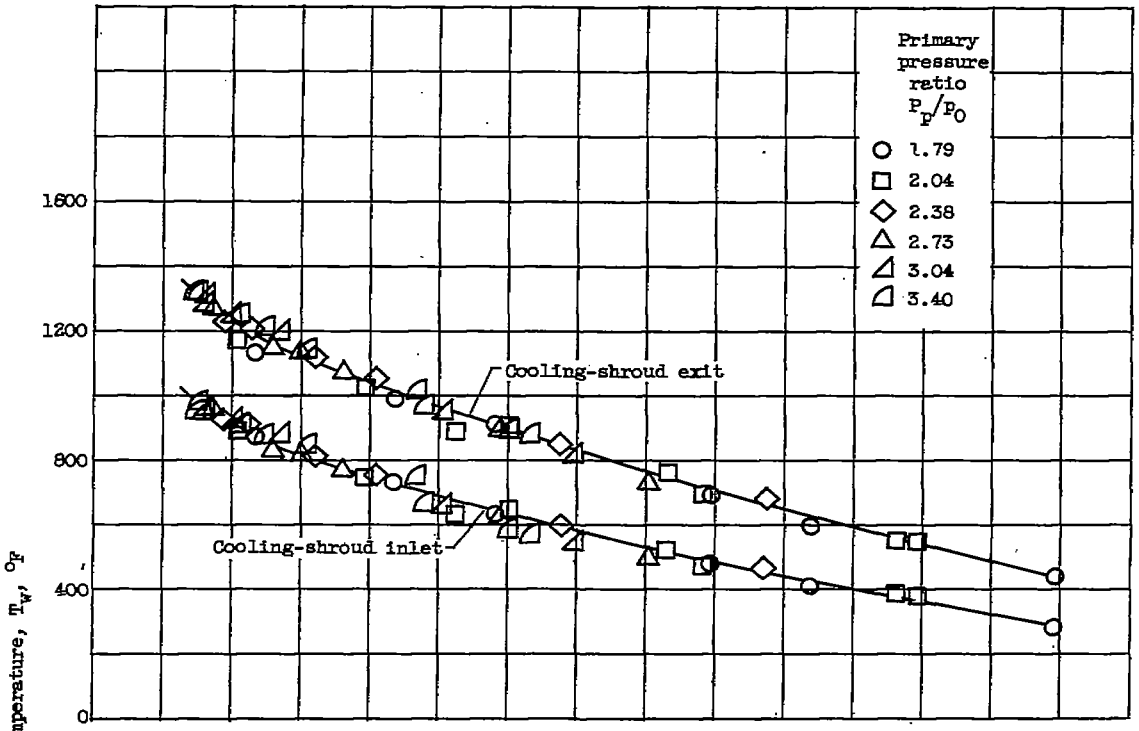

(a) Variation of afterburner shell temperature with gas-flow ratio for range of primary pressure ratio for configuration B.

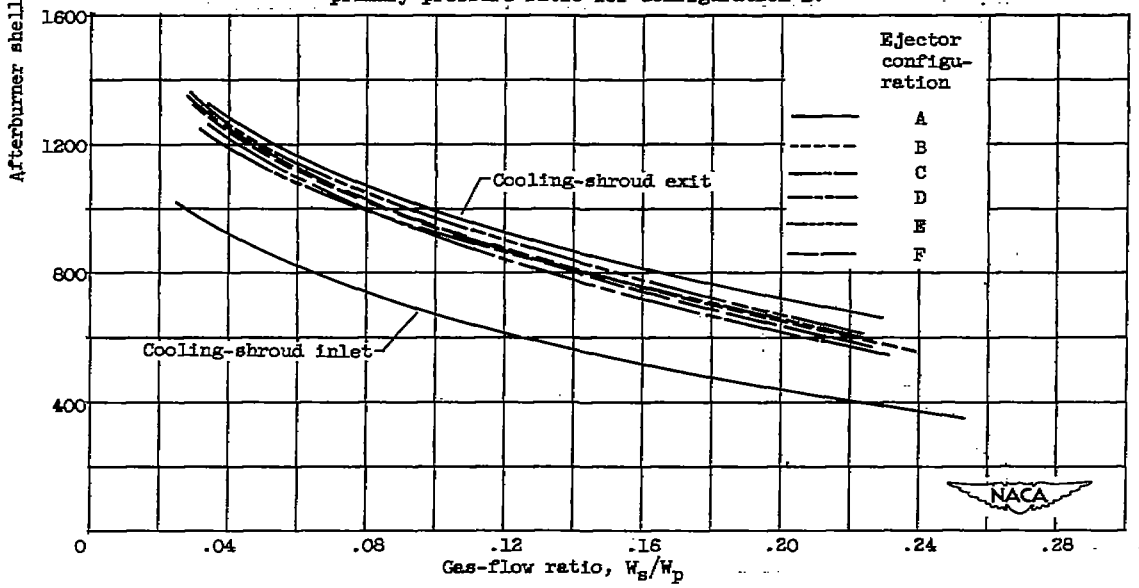

(b) Variation of afterburner shell temperature with gas-flow ratio for all configurations.

Figure 16. - Variation of afterburner shell temperature, measured at entrance and exit of cooling shroud, with gas-flow ratio.

[redacted]

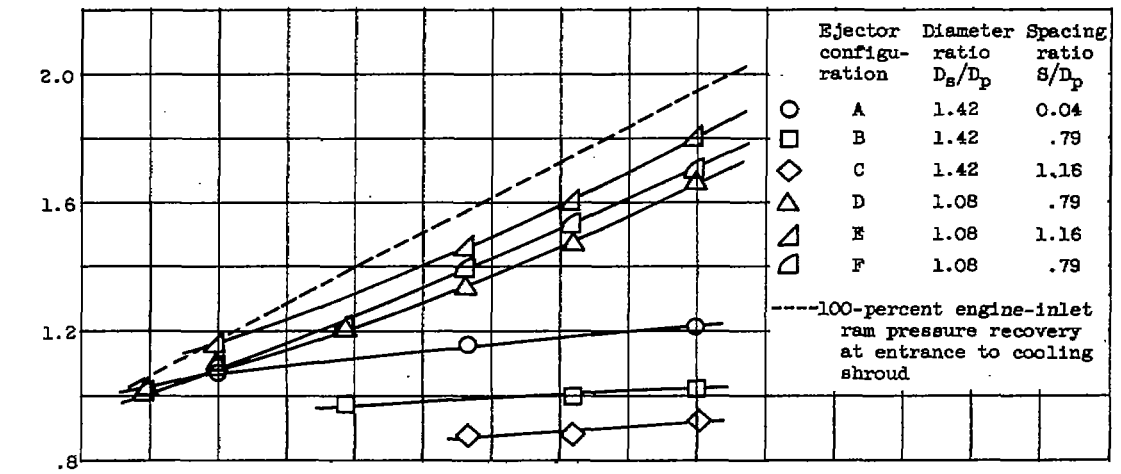

(a) Gas-flow ratio, 0.04.

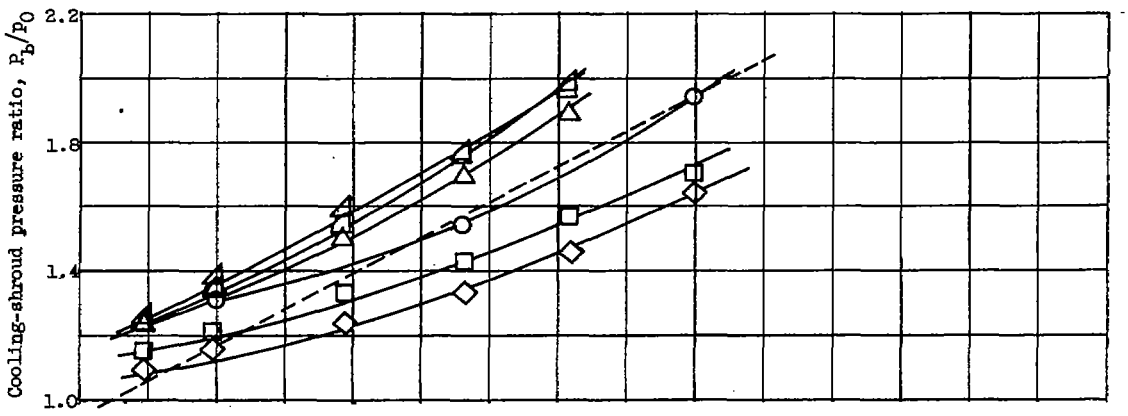

(b) Gas-flow ratio, 0.10.

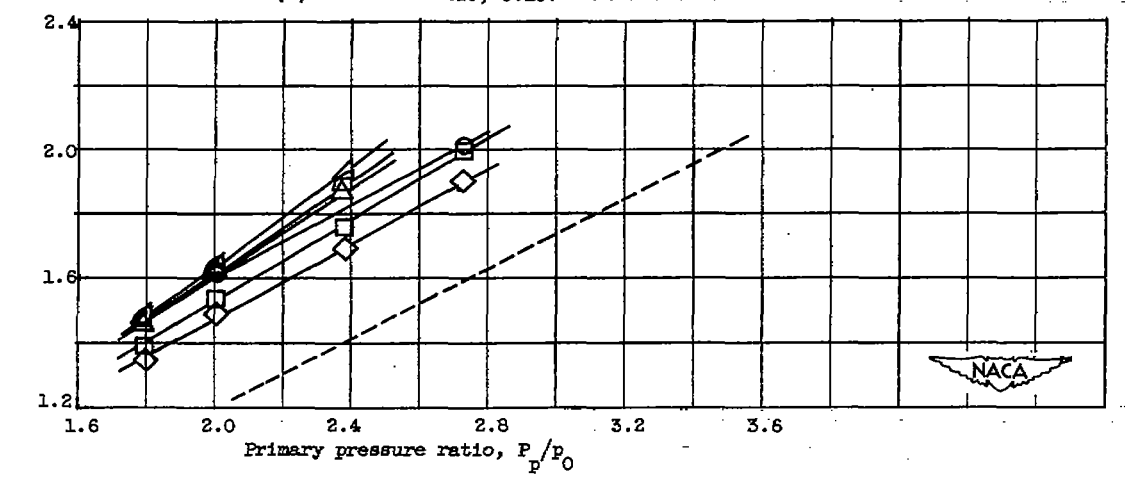

(c) Gas-flow ratio, 0.16.

Figure 17. - Variation of cooling-shroud pressure ratio with primary pressure ratio for constant gas-flow ratio.

[redacted]

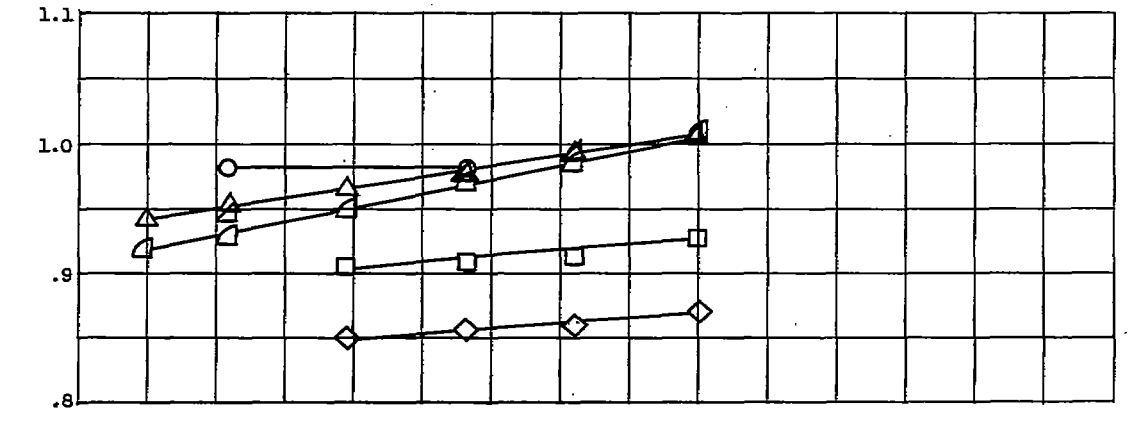

(a) Gas-flow ratio, 0.04.

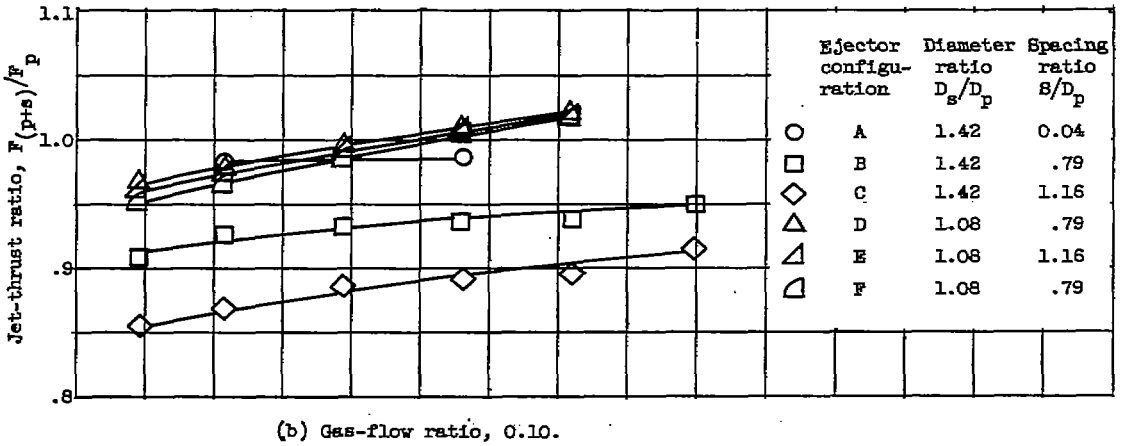

(b) Gas-flow ratio, 0.10.

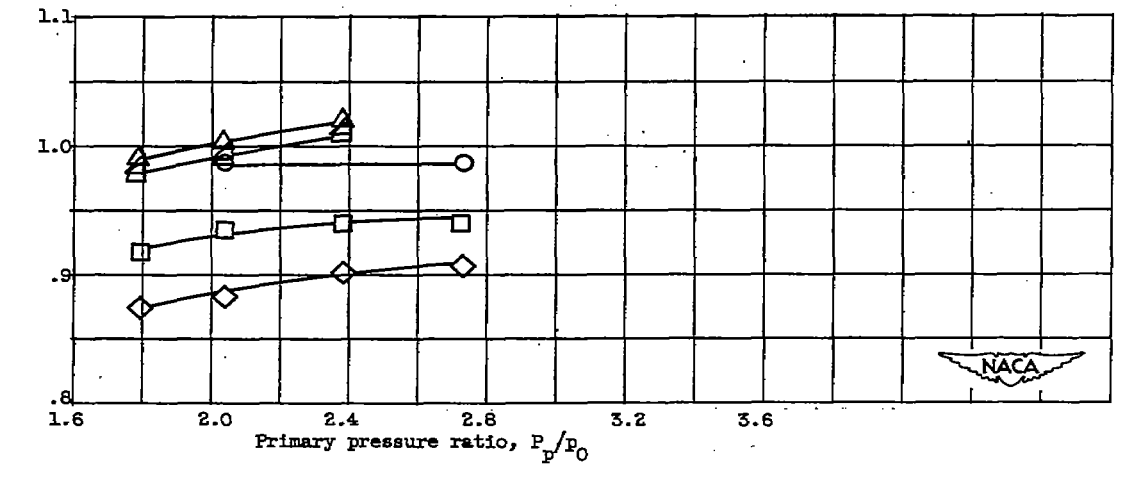

(c) Gas-flow ratio, 0.16.

Figure 18. - Variation of jet-thrust ratio with primary pressure ratio at constant gas-flow ratio.

[redacted]

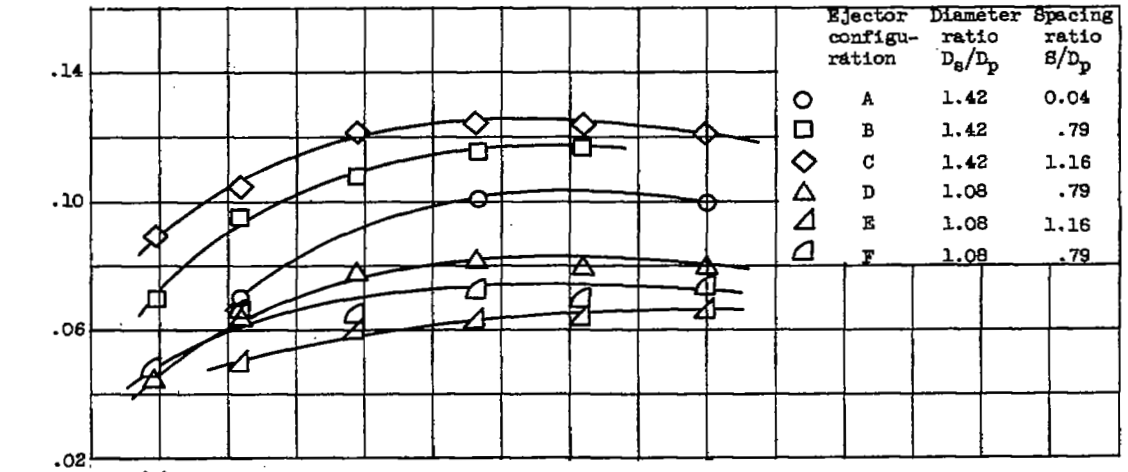

(a) 100-percent engine-inlet ram pressure recovery at entrance to cooling shroud.

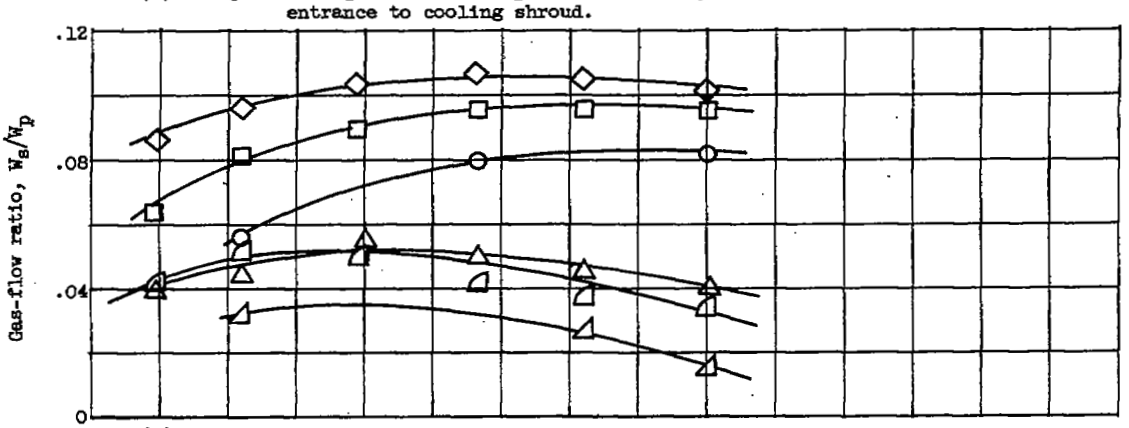

(b) 70-percent engine-inlet ram pressure recovery at entrance to cooling shroud.

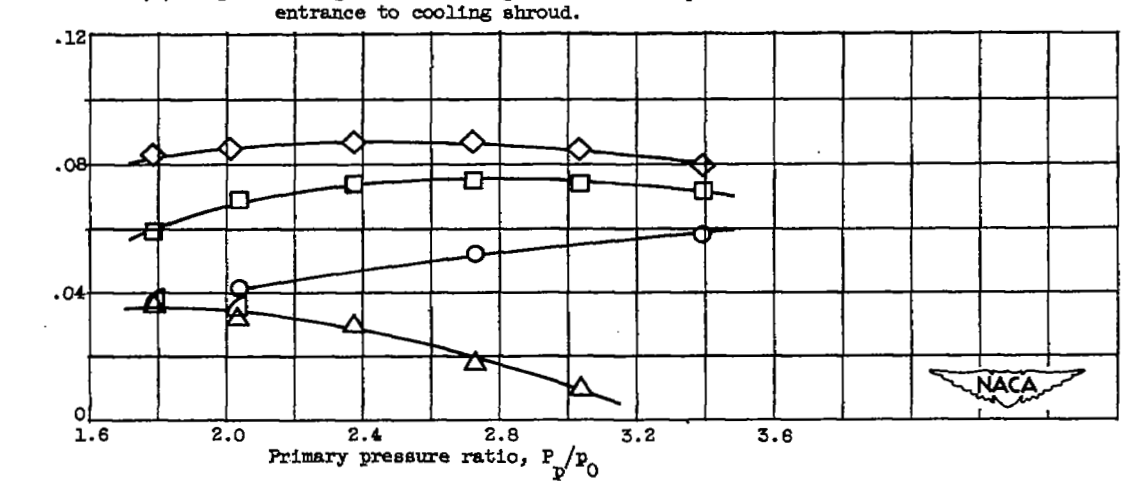

(c) 40-percent engine-inlet ram pressure recovery at entrance to cooling shroud.

Figure 19. - Variation of gas-flow ratio with primary pressure ratio for constant recoveries of engine-inlet pressure at entrance to cooling shroud.

[redacted]

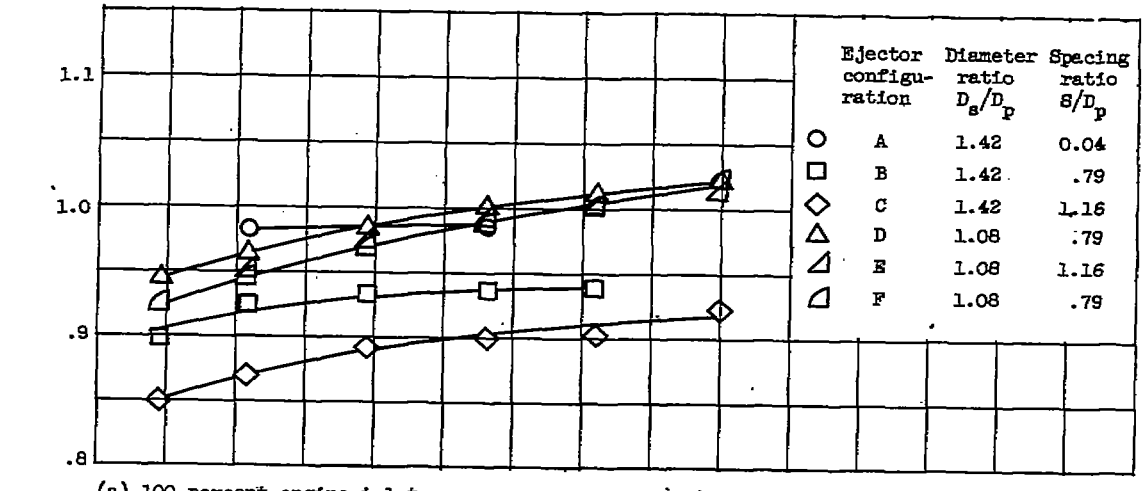

(a) 100-percent engine-inlet ram pressure recovery at entrance to cooling shroud.

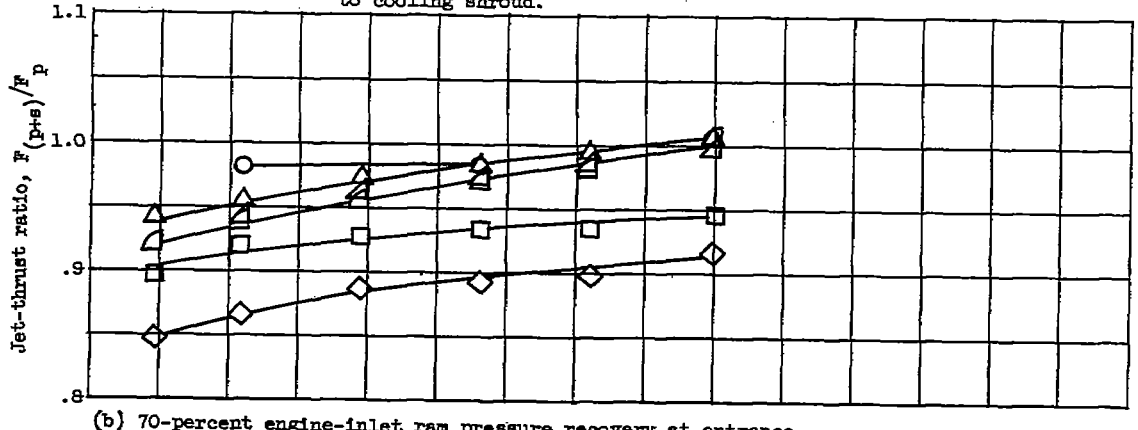

(b) 70-percent engine-inlet ram pressure recovery at entrance to cooling shroud.

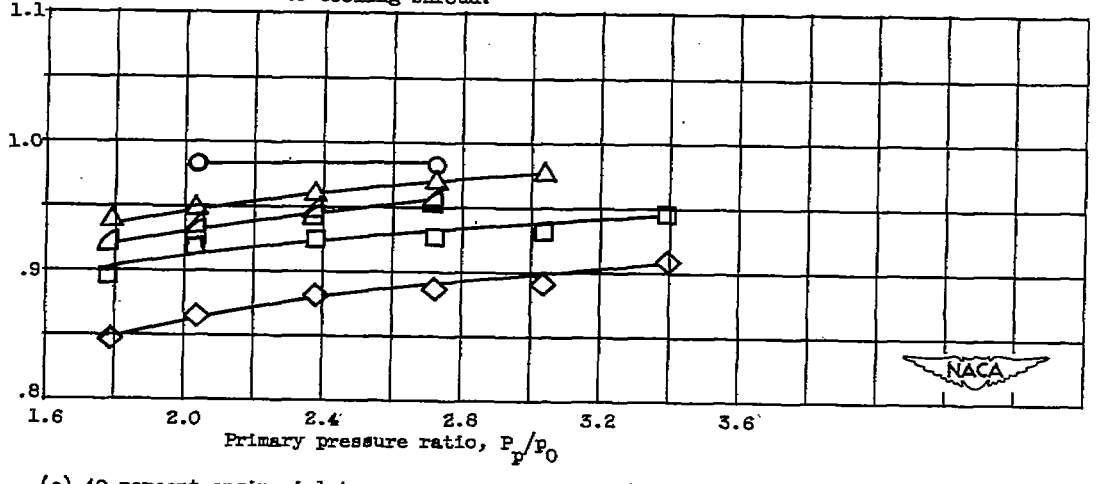

(c) 40-percent engine-inlet ram pressure recovery at entrance to cooling shroud.

Figure 20. - Variation of jet-thrust ratio with primary pressure ratio for constant recoveries of engine-inlet pressure at entrance to cooling shroud.

[redacted]

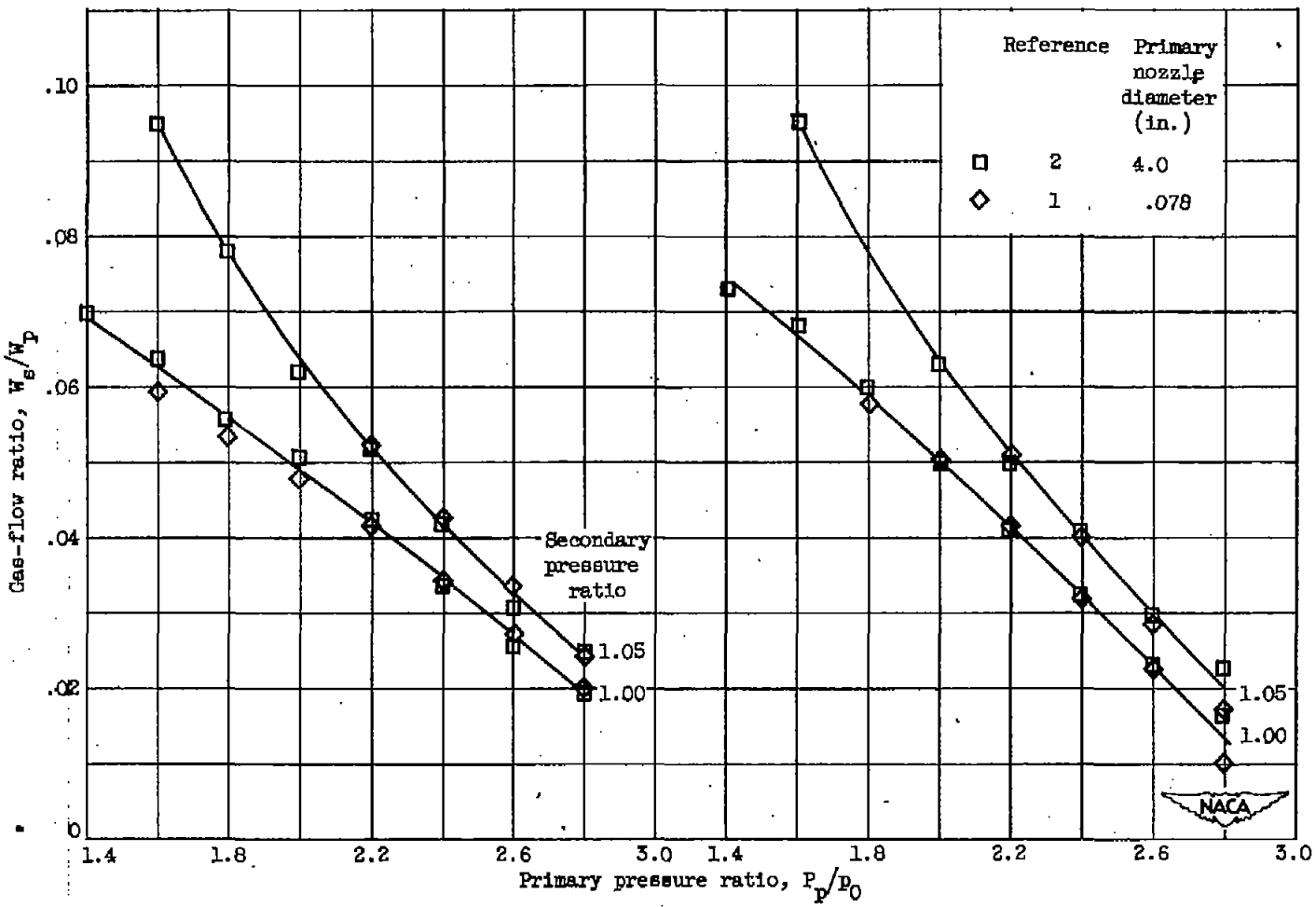

(a) Spacing ratio, 0.79. (b) Spacing ratio, 1.16.

Figure 21. - Comparison of small-scale conical-ejector data from references 1 and 2. Temperature ratio, 1.0; diameter ratio, 1.08.

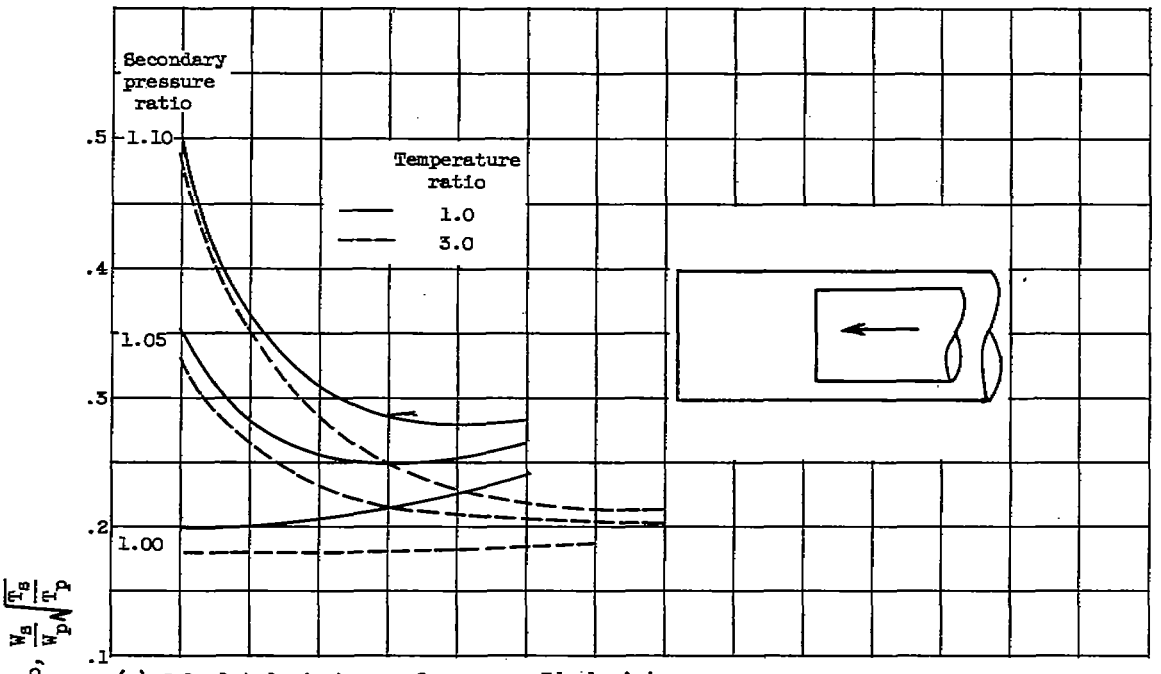

(a) Calculated ejector performance. Ideal mixing and constant static pressure assumed.

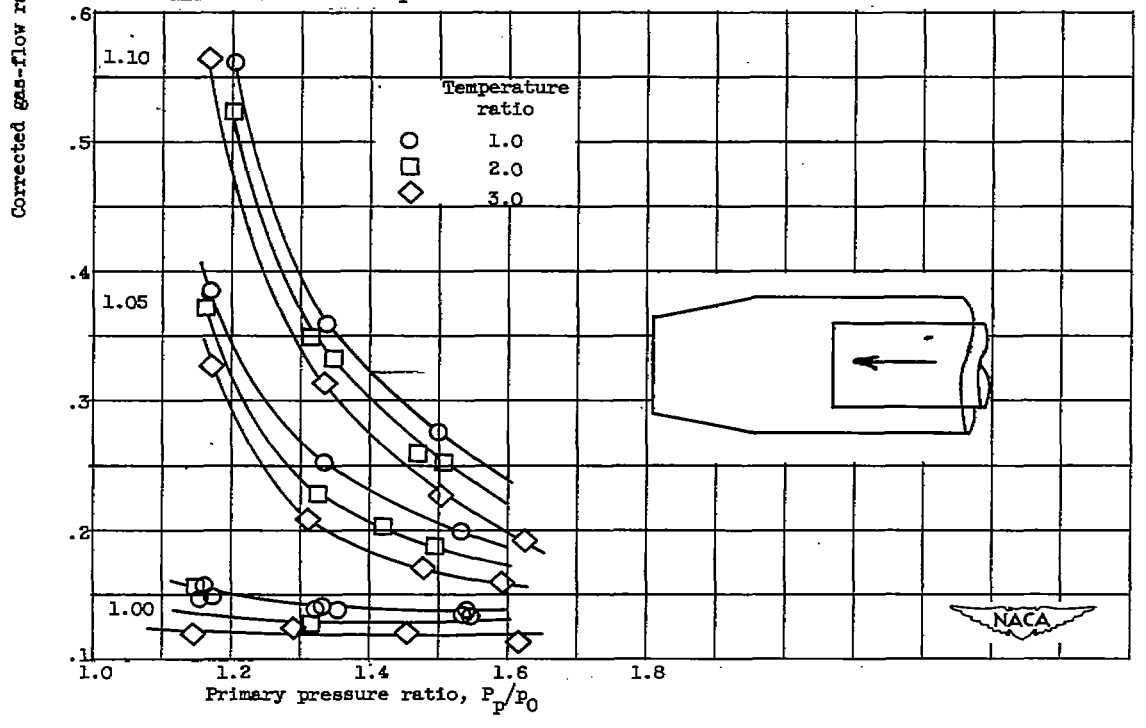

(b) Experimental ejector data. Spacing ratio, 2.50.

Figure 22. - Variation of corrected gas-flow ratio with primary pressure ratio for hypothetical ejector assuming ideal mixing and constant static pressure and for experimental ejector with same diameter ratio. Data from reference 4. Diameter ratio, 1.222.

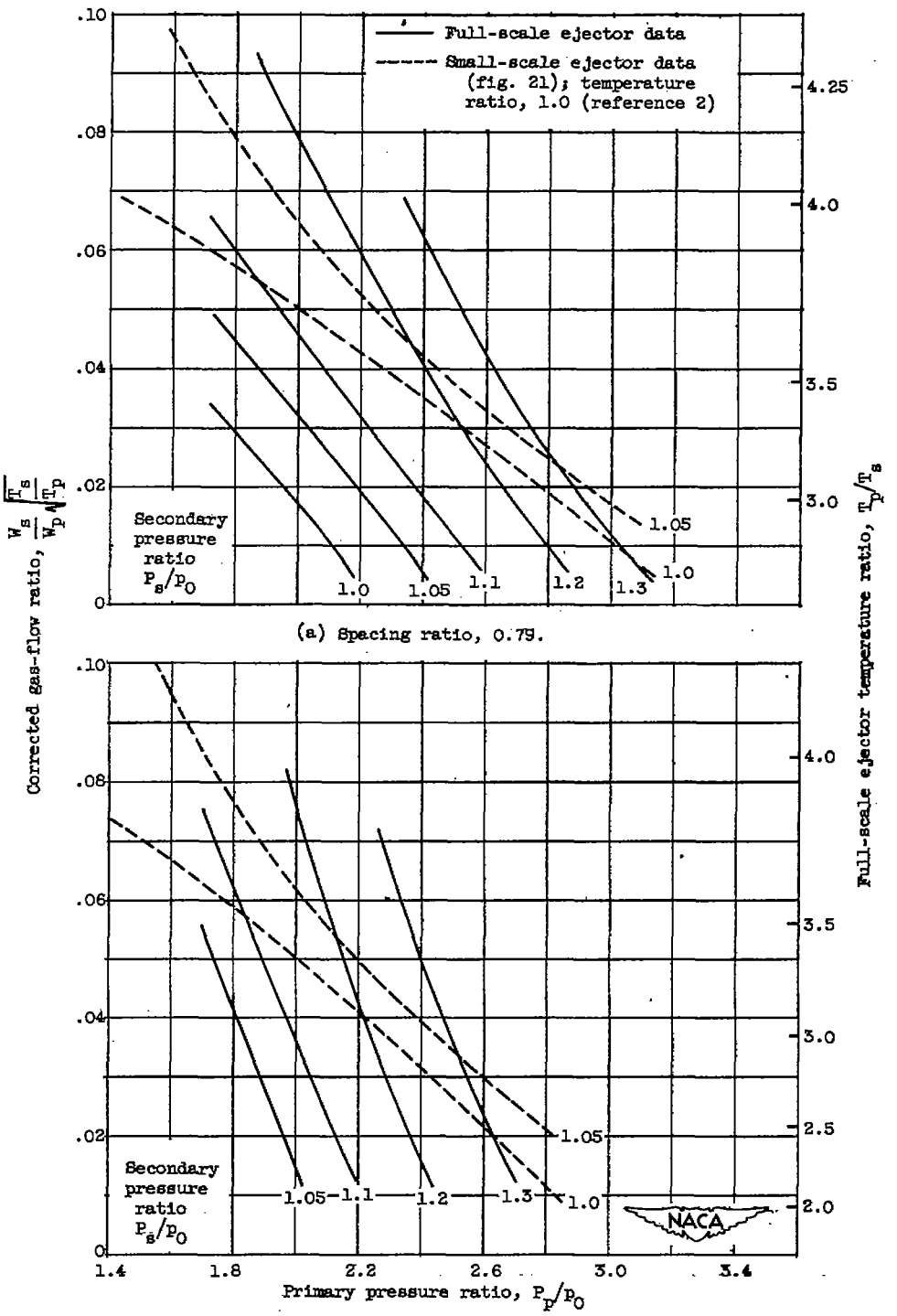

(a) Spacing ratio, 0.79.

(b) Spacing ratio, 1.16.

Figure 23. - Comparison of full-scale ejector data obtained at temperature ratios from 2 to 5 with small-scale ejector data obtained at a temperature ratio of 1.0. Diameter ratio, 1.08.